

4

AD-A228 037

Solar Cycle Effects on the Near-Earth Space Systems

Prepared by

D. J. GORNEY
Space Sciences Laboratory
Laboratory Operations
The Aerospace Corporation
El Segundo, CA 90245-4691

6 August 1990

Prepared for

SPACE SYSTEMS DIVISION
AIR FORCE SYSTEMS COMMAND
Los Angeles Air Force Base
P.O. Box 92960
Los Angeles, CA 90009-2960

APPROVED FOR PUBLIC RELEASE;
DISTRIBUTION UNLIMITED

DTIC
ELECT
NOV 02 1990
S B D

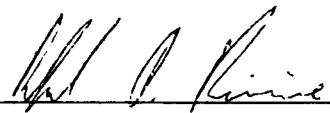
40

2

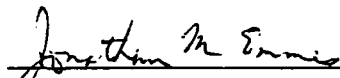
This report was submitted by The Aerospace Corporation, El Segundo, CA 90245-4691, under Contract No. F04701-88-C-0089 with the Space Systems Division, P.O. Box 92960, Los Angeles, CA 90009-2960. It was reviewed and approved for The Aerospace Corporation by H. R. Rugge, Acting Director, Space Sciences Laboratory. Captain R. Riviere was the project officer for the Mission-Oriented Investigation and Experimentation (MOIE) Program.

This report has been reviewed by the Public Affairs Office (PAS) and is releasable to the National Technical Information Service (NTIS). At NTIS, it will be available to the general public, including foreign nationals.

This technical report has been reviewed and is approved for publication. Publication of this report does not constitute Air Force approval of the report's findings or conclusions. It is published only for the exchange and stimulation of ideas.



RAFAEL A. RIVIERE, Capt, USAF
MOIE Project Officer
SSD/CNL



JONATHAN M. EMMES, MAJ, USAF
MOIE Project Manager
AFSTC/WCO OL-AB

REPORT DOCUMENTATION PAGE

1a. REPORT SECURITY CLASSIFICATION Unclassified			1b. RESTRICTIVE MARKINGS		
2a. SECURITY CLASSIFICATION AUTHORITY			3. DISTRIBUTION/AVAILABILITY OF REPORT Approved for public release; distribution unlimited.		
2b. DECLASSIFICATION/DOWNGRADING SCHEDULE					
4. PERFORMING ORGANIZATION REPORT NUMBER(S) TR-0090(5940-06)-3			5. MONITORING ORGANIZATION REPORT NUMBER(S) SSD-TR-90-25		
6a. NAME OF PERFORMING ORGANIZATION The Aerospace Corporation Laboratory Operations		6b. OFFICE SYMBOL (If applicable)	7a. NAME OF MONITORING ORGANIZATION Space Systems Division		
6c. ADDRESS (City, State, and ZIP Code) El Segundo, CA 90245-4691			7b. ADDRESS (City, State, and ZIP Code) Los Angeles Air Force Base Los Angeles, CA 90009-2960		
8a. NAME OF FUNDING/SPONSORING ORGANIZATION		8b. OFFICE SYMBOL (If applicable)	9. PROCUREMENT INSTRUMENT IDENTIFICATION NUMBER		
8c. ADDRESS (City, State, and ZIP Code)			10. SOURCE OF FUNDING NUMBERS		
PROGRAM ELEMENT NO.		PROJECT NO.	TASK NO.	WORK UNIT ACCESSION NO.	
11. TITLE (Include Security Classification) Solar Cycle Effects on the Near-Earth Space Environment					
12. PERSONAL AUTHOR(S) Gorney, David J.					
13a. TYPE OF REPORT		13b. TIME COVERED FROM _____ TO _____		14. DATE OF REPORT (Year, Month, Day) 1990 August 06	
15. PAGE COUNT 69					
16. SUPPLEMENTARY NOTATION.					
17. COSATI CODES			18. SUBJECT TERMS (Continue on reverse if necessary and identify by block number)		
FIELD	GROUP	SUB-GROUP	> Solar Flares Sunspot Cycle, Geomagnetic Storms, Solar Winds Solar Activity		
19. ABSTRACT (Continue on reverse if necessary and identify by block number)					
<p>Forecasts of the magnitude of solar activity in the 1990s (solar cycle 22) imply that the expected levels of activity might be some of the most extreme ever recorded, and almost certainly the levels of activity will be the highest experienced during the space age. Even as early as one year before the expected maximum of solar cycle 22 in 1990, unprecedented levels of solar activity (for example, the solar flares and solar particle events of August-October 1989) and geomagnetic activity (for example, the auroral events and geomagnetic storms of March 1989) have been observed. These solar and geophysical events have stirred scientific interest in both the long-term behavior of solar activity and in the physics which couples the energy of solar events to the near-Earth environment. Furthermore, the operational community (including those involved in satellite operations, telephone and radio communication, electric power distribution, aviation, and others) have experienced many adverse effects of these solar and geophysical events. Many more episodes of activity are expected throughout the upcoming 4-5 years. The purpose of this report is to review the direct and indirect influences of solar activity on the near-Earth environment and to describe some of the implications of the high levels of solar activity which are expected to occur in the 1990-1994 time period.</p>					
20. DISTRIBUTION/AVAILABILITY OF ABSTRACT <input checked="" type="checkbox"/> UNCLASSIFIED/UNLIMITED <input type="checkbox"/> SAME AS RPT. <input type="checkbox"/> DTIC USERS			21. ABSTRACT SECURITY CLASSIFICATION Unclassified		
22a. NAME OF RESPONSIBLE INDIVIDUAL			22b. TELEPHONE (Include Area Code)		22c. OFFICE SYMBOL

PREFACE

The author benefitted greatly from discussions and data shared by Joe Allen, Dan Wilkinson, Joann Joselyn, Gary Heckman, Don Smart, Peggy Shea, Joan Feynman, Al Vampola, and Richard Walterscheid.

Accession For	
NTIS GRA&I	<input checked="" type="checkbox"/>
DTIC TAB	<input type="checkbox"/>
Unannounced	<input type="checkbox"/>
Justification	
By	
Distribution/	
Availability Codes	
Dist	Avail and/or Special
A-1	

CONTENTS

PREFACE.....	1
1. INTRODUCTION.....	7
2. EFFECTS OF SOLAR ACTIVITY ON THE NEAR-EARTH ENVIRONMENT.....	11
2.1 Solar Particle Events.....	12
2.2 Geomagnetic Activity.....	21
2.3 The Neutral Atmosphere.....	33
2.4 The Ionosphere.....	36
2.5 Magnetospheric Plasmas.....	45
2.6 Magnetospheric Energetic Particles.....	49
3. FORECASTS FOR SOLAR CYCLE 22.....	53
4. SUMMARY.....	57
REFERENCES.....	59
GLOSSARY OF SPECIAL SYMBOLS.....	69

FIGURES

1.	A Historic Record of Sunspot Activity, Including Data Through 1989.....	8
2.	A Logarithmic Plot of the Typical Time Evolution of a Solar Particle Event Observed at Earth.....	14
3.	A Polar View of Interplanetary Space in the Ecliptic Plane, Showing the Propagation of Solar X-Rays, Solar Energetic Particles, and the Solar Wind from the Sun to the Vicinity of the Earth.....	16
4.	A Superimposed Epoch Representation of the Yearly Fluence of >30 MeV Solar Protons as a Function of Time Relative to the Year of Sunspot Maximum.....	18
5.	Examples of Three Intense Solar Proton Events Observed over the Past Three Solar Cycles.....	20
6.	Annual Averages of Sunspot Number and Geomagnetic Activity Index from 1870 to 1979.....	22
7.	Annual Averages of the Geomagnetic Activity vs Sunspot Number.....	24
8.	Histograms of Solar Wind Speed Distributions for the Years 1962-1974.....	26
9.	A Plot of Six-Month Averages of the Solar Wind Speed and the Geomagnetic Activity Index for the Time Period Spanning 1962-1975.....	28
10.	Examples of Energy Coupling in a Purely Driven System, a Purely Triggered System, and a Complex System.....	31
11.	A Plot of Satellite Lifetimes vs Solar 10.7 cm Radio Flux for Several Initial Altitudes from 300 km to 800 km.....	37
12.	Histograms of the Occurrence Frequency of Signal Fades at Thule, Greenland Compared to Monthly-Average Sunspot Number from 1979 to 1986.....	43
13.	Local-Time-Latitude Plots of the Regions and Severity of Signal Fades During Solar Maximum and Minimum Periods.....	44

14.	A Meridional View of the Earth's Magnetosphere Showing the Key Plasma and Energetic Particle Populations Which Respond to Variations in Solar Wind Parameters.....	46
15.	A Plot of Observed Smoothed Sunspot Numbers Compared to Values Predicted Using the McNish-Lincoln Technique.....	56

TABLES

1.	Empirical and Theoretical Relationships Between Geomagnetic Activity and Solar Wind Parameters.....	29
2.	Empirical Relationships Between Solar-Geomagnetic Activity Indices and Ionospheric Parameters.....	41

1. INTRODUCTION

The regular variation of solar activity, which has come to be known as the 11-year sunspot cycle, was discovered in the mid-19th century (Schwabe, 1849), although documented scientific observations of the existence of cyclic behavior extend as far back as the invention of the telescope in the 17th century (see Galilei, 1957). Perhaps the earliest recorded physical effects of solar activity on man were intermittent telegraph outages in the late 1850s (Maggs, 1988), although it was not until the 1940s that systematic scientific observations of particulate emissions from the sun were made at Earth (e.g., Forbush, 1946, 1950; also see Lovell, 1987; Smart and Shea, 1989).

A historic record of sunspot activity, including data through 1989, is shown in Figure 1. Solar physicists have predicted that the upcoming maximum of solar activity, scheduled to occur in 1990, might be the most extreme ever recorded (e.g., Hirman et al., 1988; Kane, 1987; Lantos and Simon, 1987; Schatten and Sofia, 1987; Thompson, 1988; Withbroe, 1989). Extreme levels of solar and geomagnetic activity observed in 1989 seem to confirm these predictions (see Allen et al., 1989). A power outage in Eastern Canada caused by an extreme geomagnetic event in March 1989 (affecting approximately 6 million people for over 9 hours) speaks to the practical importance of these phenomena. It seems certain, based on the observed rate of increase in solar activity starting with the most recent minimum in September 1986 (the start of solar cycle 22), that the upcoming solar maximum will be the most severe of those which have occurred during the space age (i.e., solar cycles 20-22). Thus, solar cycle 22 represents a unique opportunity for geophysicists to observe the solar-terrestrial system in one of its most extreme conditions.

Correlations between solar activity and disturbances in the near-Earth magnetosphere, ionosphere, and atmosphere are well documented. Unfortunately, because of the complex and sometimes indirect interactions between the sun and the near-Earth space environment (e.g., Akasofu, 1981; Crooker

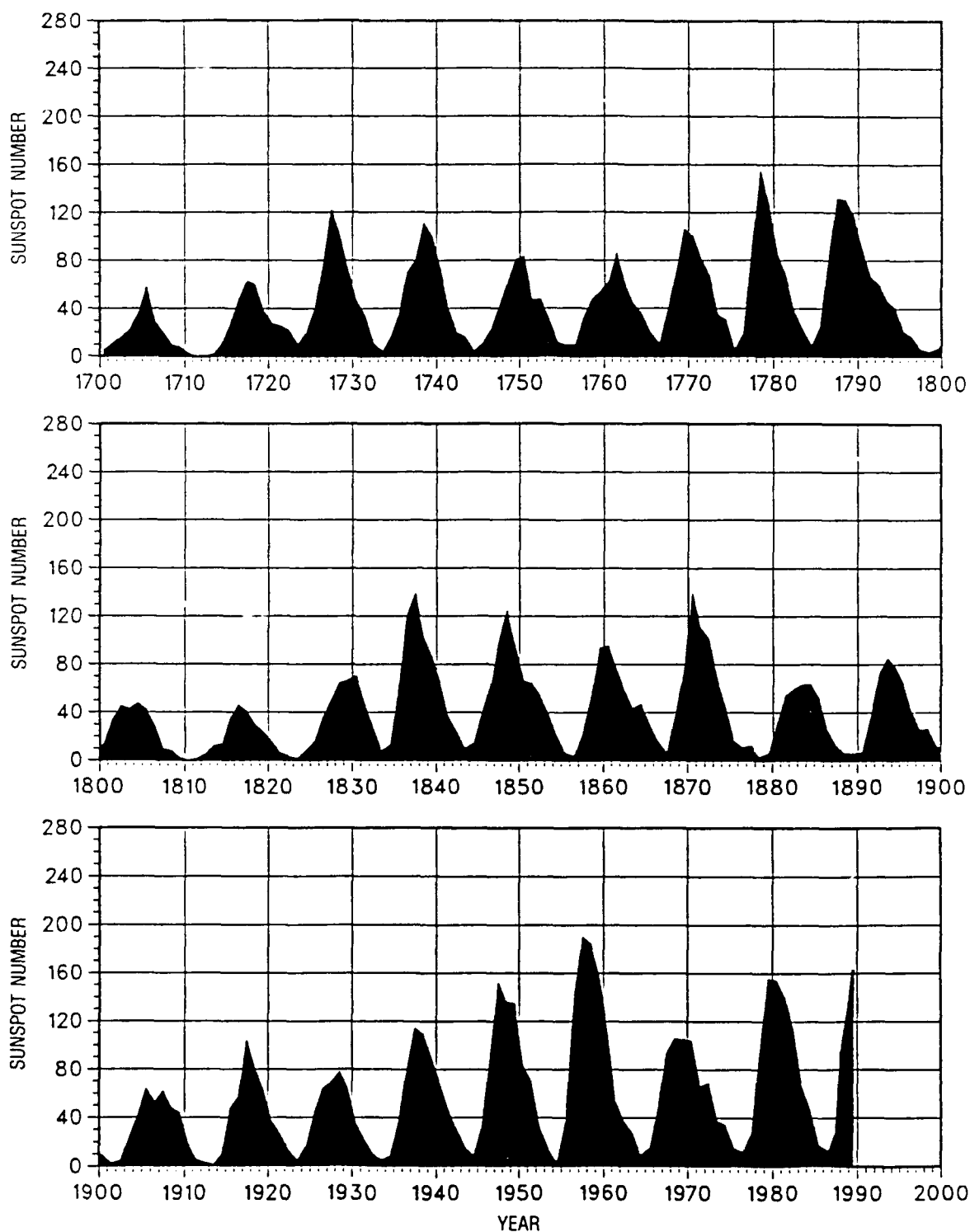


Figure 1. A Historic Record of Sunspot Activity, Including Data Through 1989. The value plotted is the 13-month smoothed sunspot number. Data are from the NOAA National Geophysical Data Center.

and Siscoe, 1986), very few long-term quantitative predictions can be made regarding the expected effects of an extreme solar maximum on the near-Earth environment or on the complex systems operating in that environment. Indeed, the scientific knowledge and practical experience gained over the past three solar cycles have not yet yielded an adequate state-of-the-art capability for short-term forecasting of the occurrence of geomagnetic storms based on real-time observations of solar activity (J. Joselyn, private communication, 1989). However, progress is being made in this area, and a number of important qualitative predictions can be made with high confidence (see Feynman and Gu, 1986).

The effects of solar activity on near-Earth plasmas and, in turn, on man-made systems are quite varied in magnitude, timescale, and predictability. It is reasonable to classify the effects into two categories: (1) direct abrupt effects, usually caused by rapid changes in solar UV and x-ray illumination of the Earth's atmosphere and ionosphere during solar flares, and (2) indirect effects which are caused by more complex interactions between the solar wind and the coupled magnetosphere-ionosphere-atmosphere system. The direct effects can be understood more easily, but they are not necessarily any more predictable. Certainly the frequency of occurrence (though not necessarily the severity) of optical and x-ray flares and solar proton events correlates well with the 11-year sunspot cycle (see Hirman et al., 1988), and an extreme solar maximum almost certainly would involve more major flare occurrences. Typically the magnitude of the "background" solar UV flux tracks the sunspot number and solar radio flux fairly well. For 13-month smoothed data, the following linear relationship (Wilson, 1984; Withbroe, 1989) between the 10.7 cm radio flux ($F_{10.7}$) and the sunspot number (R) can be used:

$$R = 1.075 F_{10.7} - 61.1. \quad (1)$$

($F_{10.7}$ represents the solar radio flux in units of 10^{-22} Watts/m² Hz at 10.7cm wavelength.) On the other hand, the total visible radiation from the sun varies only slightly (<0.2%) during occurrences of large sunspot

groups. Solar luminosity tends to peak near sunspot maximum. The bright, active regions on the sun tend to increase in intensity enough to offset the growth in area of the darker sunspot groups (see Coffey, 1989) during sunspot maximum years. The relationship between the solar cycle and the physical parameters of the solar wind which (indirectly) cause geomagnetic disturbances at the Earth is more complex, however.

The purpose of this report is to review the direct and indirect influences of solar activity on the near-Earth space environment and to point out some of the expected effects of solar activity on systems which operate within that environment. The review concentrates on those major areas where our current physical understanding can lead to firm predictions of the expected effects of solar activity (in particular, extremely intense solar activity) on the near-Earth space environment. The review is not exhaustive, but attempts to provide sufficient reference material for the reader to be able to acquire additional information on topics which can be covered only briefly here. An attempt has also been made to maintain an historical perspective while including some up-to-date data and recent results.

This report is divided into four major sections, including this introduction. Section 2 describes direct and indirect effects of solar activity on the near-Earth environment. Solar proton events and the effects of solar illumination on the ionosphere and neutral atmosphere are discussed as examples of direct effects. Geomagnetic storms, auroral activity, and the trapped particle environment are discussed as examples of indirect effects. Weather and climatological effects are specifically excluded from this review, as those topics require special attention in their own right. Section 3 provides a review of predictions for the current solar cycle 22. Section 4 offers a summary which is intended to address the general question of what might be expected as a result of possible extreme levels of solar activity in the 1990s. A glossary of special symbols appears at the end of the text.

2. EFFECTS OF SOLAR ACTIVITY ON THE NEAR-EARTH ENVIRONMENT

Solar activity directly affects the Earth's neutral atmosphere at virtually all altitudes. The Earth's neutral atmosphere includes not only the air which we breathe at low altitudes, but also a high-altitude extension known as the thermosphere. Variations in the neutral atmosphere are more dramatic and occur on shorter time scales with increasing atmospheric altitudes, including altitudes where low-Earth-orbiting satellites fly (see Walterscheid, 1989). These effects have significant operational effects on vehicles flying through these regions and on systems which must track and monitor satellites and space debris. Energetic charged particles emitted from the sun during some solar flares can cause upsets in microelectronic devices on satellites; can affect radio propagation through the atmosphere; and can pose a threat to humans in space. Man-made electrical, satellite, and communications systems are affected strongly by the near-Earth plasma environments which comprise the ionospheric and magnetospheric regions. Plasmas within the ionosphere, at altitudes from 50-1500 km, arise from the ionization of neutral atmospheric atoms and molecules by solar illumination and by the precipitation of energetic charged particles (ions and electrons) from space. Plasmas in the magnetospheric region are comprised of ions and electrons which are energized, distributed, and confined out to distances of many Earth radii by complex dynamical interactions between the Earth's own magnetic field, the ionosphere, and the magnetized solar wind. Thus, the sun (including its light output, its magnetic configuration, and its output of solar wind), the magnetosphere, the ionosphere, and the atmosphere are a coupled physical system, whose responses to changes in solar activity are pervasive and complex (see Gorney, 1989). Man-made systems typically interact with a very small segment of this coupled system, and it can be very difficult to draw a straight line between cause and effect for individual events or measurements. The goal of this section is to summarize the major cause-and-effect relationships between solar activity and conditions in the Earth's atmosphere, ionosphere, and magnetosphere.

2.1 SOLAR PARTICLE EVENTS

One of the most direct influences of solar activity on the near-Earth space environment is the sporadic occurrence of very energetic (10 MeV to above a GeV) solar particle events in association with solar flares (see Smart and Shea, 1985, 1989). Although solar particle events are fairly infrequent (on average, only a few events occur per year), these events represent the most energetic tangible manifestations of solar activity, and the events have important consequences for the near-Earth environment and for man-made systems operating within that environment. The first observations of solar particle emissions reaching the Earth's surface were made in the 1940s (e.g., Forbush, 1946, 1950), but it was not until the mid-1950s that methodical and relatively continuous monitoring was initiated. Most of the early observations of solar particle events were indirect in the sense that they detected either secondary particles resulting from the impact of the primary solar particles on the Earth's upper atmosphere or the effects of changes in atmospheric ionization caused by the impact of the solar particles on the polar atmosphere.

The ground-based particle detection techniques employed muon detectors (sensitive to secondary particles resulting from the interaction of several GeV protons in the atmosphere) and later, neutron monitors (see Simpson, 1957; Carmichael, 1968) which were sensitive to secondary particles from the atmospheric interaction of solar protons having energies of several hundred MeV and above. Solar particle events registered by these ground-based particle detectors thus involved solar protons of relativistic energies, and the events which were recorded have come to be known as "relativistic proton events" or "ground level events" (sometimes abbreviated as GLEs).

Radio receivers monitoring the propagation of galactic radio "noise" through the Earth's ionosphere proved to be very sensitive to modifications of the ionosphere caused by the impact of solar particles. These monitoring receivers (see Little and Leinbach, 1959), generally called "radio ionospheric opacity meters" (riometer, for short), responded with high

sensitivity to the impact of relatively low energy solar particles (~ 1 -10 MeV), and the events they recorded are called "polar cap absorption events" or PCAs. Because of the indirect nature of these ground-based measurements, it is not possible to derive detailed information on the primary solar particle event energy spectrum or composition, although some estimates of the hardness of the spectra and the intensity of the events can be determined. Nevertheless, since neutron monitors and riometers have been in continuous operation for several decades, these data sets provide extremely useful information on the long-term historical occurrence patterns for solar proton events.

It was not until the advent of the space age that direct observations of the spectra and composition of solar particle events were accomplished routinely (see Gloeckler, 1979; Cook et al., 1984; McGuire et al., 1986; Mason, 1987 for recent results and reviews). Coincidentally, the adverse effects of solar particle events on electronic subsystems on satellites and health considerations for humans in space represented important practical needs for acquiring detailed knowledge of the characteristics of these events and for developing estimates of "worst-case" environments. Based on space-based observations of solar particle events, the elemental abundances of solar particle events are now documented fairly well (see Table 1 of Smart and Shea, 1989), at least up to energies of a few 10s of MeV. Also, the time evolution of individual solar particle events and their long-term variations over several solar cycles have been studied.

Figure 2 shows the typical time evolution of a solar particle event observed in the vicinity of the Earth. Details of this time-evolution profile depend on the time evolution of the originating solar flare (see Svestka, 1976); the time scale associated with diffusion of the energetic particles within the solar corona; and the propagation of the particles within the interplanetary medium. The time evolution of the originating solar flare is observable by monitoring either the light emission from the flare or the soft x-ray emission. A reasonable correlation tends to exist between the intensity of a particle event and the intensity and duration of the originating solar flare as observed in soft x rays. Protons of

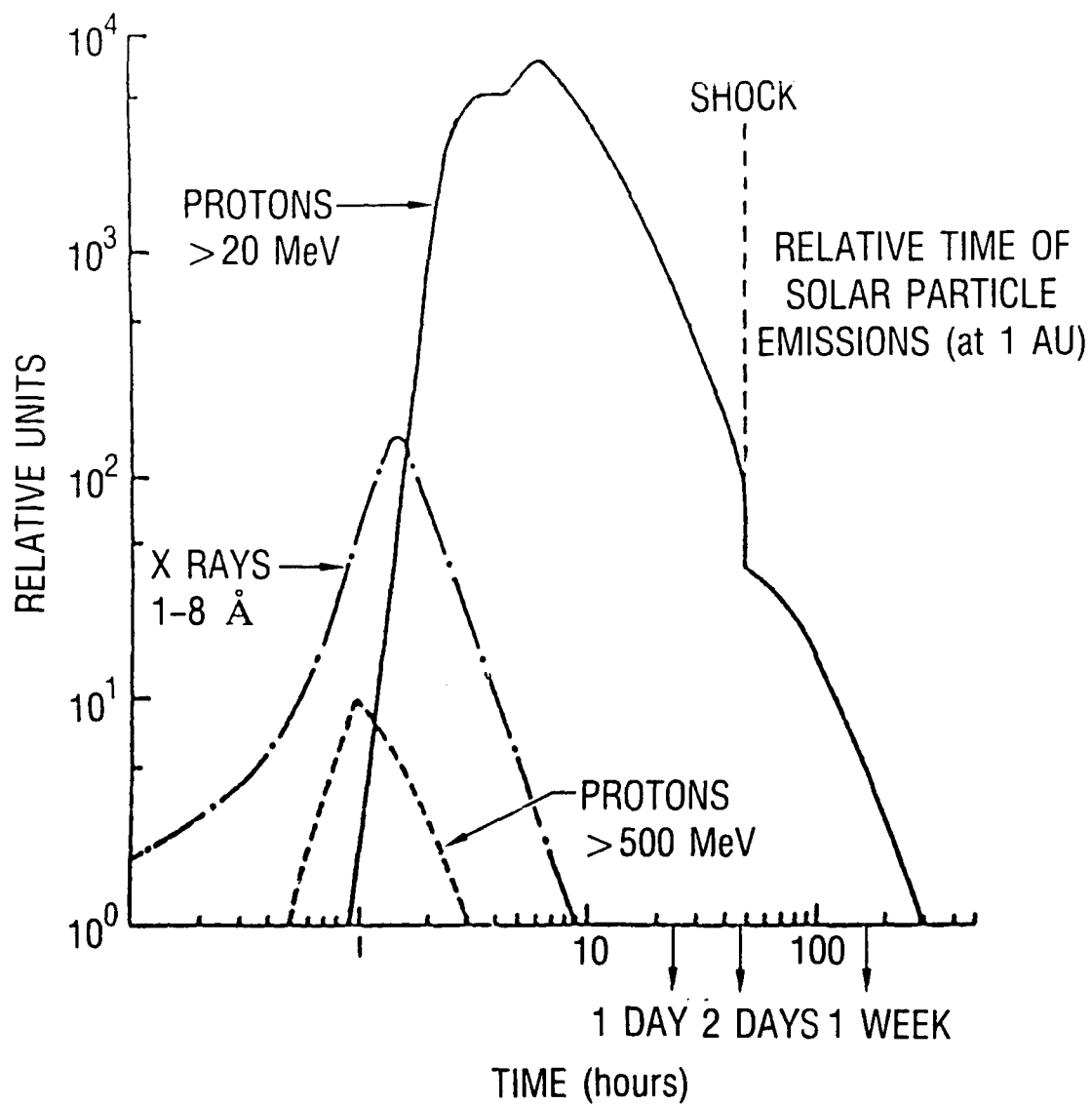


Figure 2. A Logarithmic Plot of the Typical Time Evolution of a Solar Particle Event Observed at Earth. (From Smart and Shea, 1989.)

relativistic energies generally arrive at Earth within seconds or minutes of these "line-of-sight" emissions. For high-energy particles, interplanetary propagation is generally along the magnetic field in the Archimedian spiral pattern shown in Figure 3, although the actual interplanetary field can be highly irregular, leading to much more complex time variations in flux than those depicted in Figure 2. Lower energy (~ 10 s of MeV) protons arrive with appropriate time-of-flight delays, and their distribution in time tends to be influenced greatly by diffusion within the solar corona and within the interplanetary medium. After the occurrence of a solar particle event, proton fluxes tend to decay to background values over a several-day time period.

The overall importance of an individual event depends on the maximum intensity of the event, the length of the event (which establishes the time-integrated particle flux, or fluence), the relative abundance of the higher energy component, and the relative abundance of heavy nuclei. Aside from its elemental composition, virtually all of the important characteristics of a solar particle event are influenced strongly by the location (in longitude, primarily) of the originating solar flare relative to the footprint of the interplanetary magnetic field line which is instantaneously "connected" to Earth (see Figure 3). Solar flares of similar intensity tend to give rise to particle flux at Earth that is diminished by about a factor of 10 for a ~ 1 radian displacement in solar longitude from the directly connected longitude. For typical solar wind conditions, the directly connected longitude on the sun tends to lie between about 30° and 50° west of the sun's central meridian, as viewed from the Earth.

Because of their episodic nature and the important influences of location, propagation, and diffusion on the relative magnitude of their near-Earth effects, individual solar particle events are not well correlated with "full-disk" indices of solar activity such as sunspot number or radio flux. However, a general modulation of the frequency of occurrence of solar particle events in phase with the sunspot cycle seems to be apparent in data acquired over the cycles 19-21 (see Smart and Shea, 1989, Figure 14). The occurrence frequency of proton events tends to peak

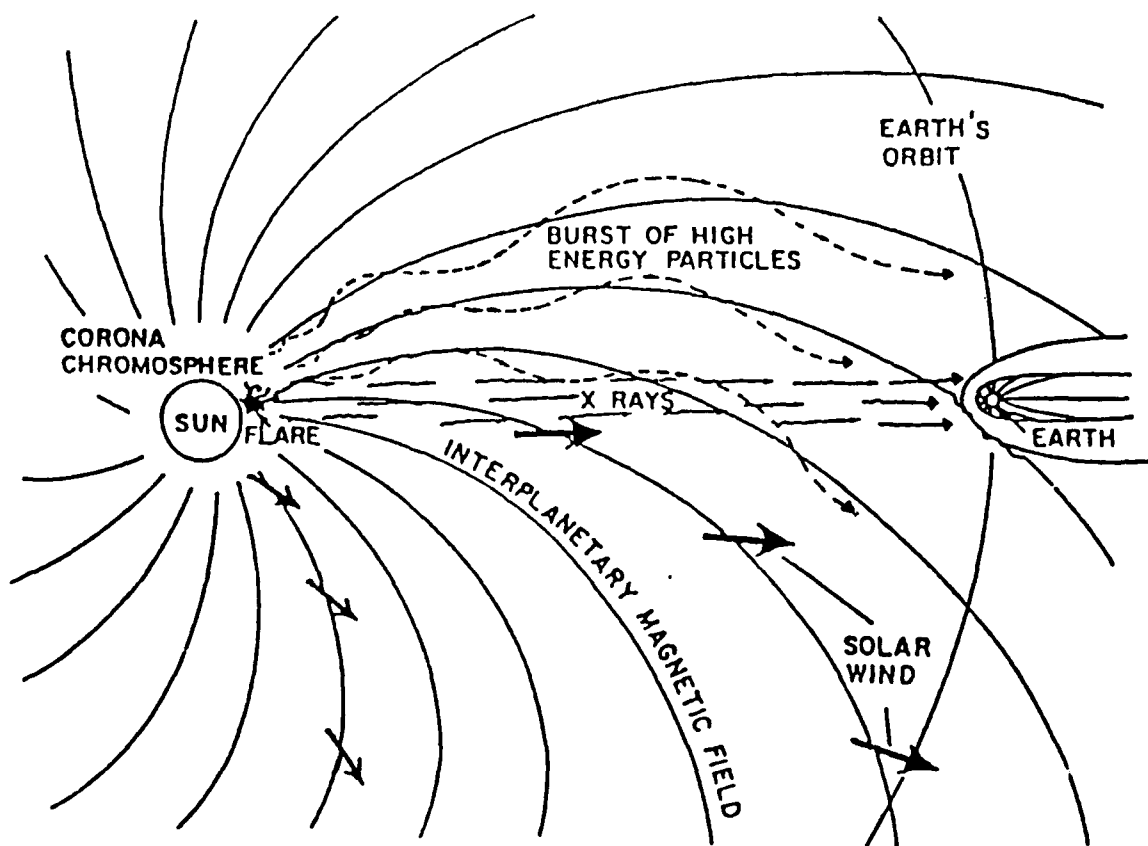


Figure 3. A Polar View of Interplanetary Space in the Ecliptic Plane, Showing the Propagation of Solar X Rays, Solar Energetic Particles, and the Solar Wind from the Sun to the Vicinity of the Earth. The sun's rotational velocity, coupled with the outward velocity of the solar wind, produces the Archimedean spiral pattern of the interplanetary magnetic field.

within a period extending from two years before to four years after the sunspot maximum, and proton event occurrence is greatly diminished during the few years surrounding sunspot minimum. Generally, the distribution of proton events tends to be broader in time than the distribution of sunspot number, and very intense events can occur virtually any time within the sunspot cycle except at minimum (Feynman, 1988).

An interesting characteristic of the largest solar particle events is that their relative intensities tend to obey a log-normal distribution (King, 1974; Feynman and Gabriel, 1990). This characteristic leads to the interesting result that one or two individual events can dominate the total proton fluence (the time-integrated flux) observed over a complete solar cycle. This behavior is shown in Figure 4 (from Zwickl and Kunches, 1989) for cycles 19-21 and the first few years of cycle 22. Figure 4 plots the yearly fluence of solar protons with energies above 30 MeV as a function of epoch relative to the year of sunspot maximum. The plot, on a logarithmic scale, shows that the proton fluence can exhibit order-of-magnitude variations from year to year, even within a single cycle. This feature is perhaps most evident for the data from cycle 22, in which more than a factor of 100 variation in proton fluence was observed between the two years preceding sunspot maximum. The dramatic increase in fluence in cycle 22 was due primarily to the occurrence of one or two extremely large events during 1989. Even with the large year-to-year variations which are evident in Figure 4, the data still demonstrate a tendency for higher fluences to occur within a few years of sunspot maximum. It is also interesting to note that the cycles with the highest sunspot numbers (e.g., cycles 19 and 22) also appear to have higher levels of integrated proton fluences.

Although over 200 solar proton events (with fluxes over $10/\text{cm}^2 \text{ sec}$ ster) have occurred over the past 30 years, only about 30 of these events have had sufficient flux at high energies to be classified as ground-level events (Smart and Shea, 1989). Furthermore, the integrated proton fluence over the same 30-year period is dominated by only a handful of events. The sporadic occurrence of these events, coupled with the logarithmic flux distribution of events, leads to great difficulty in formulating estimates

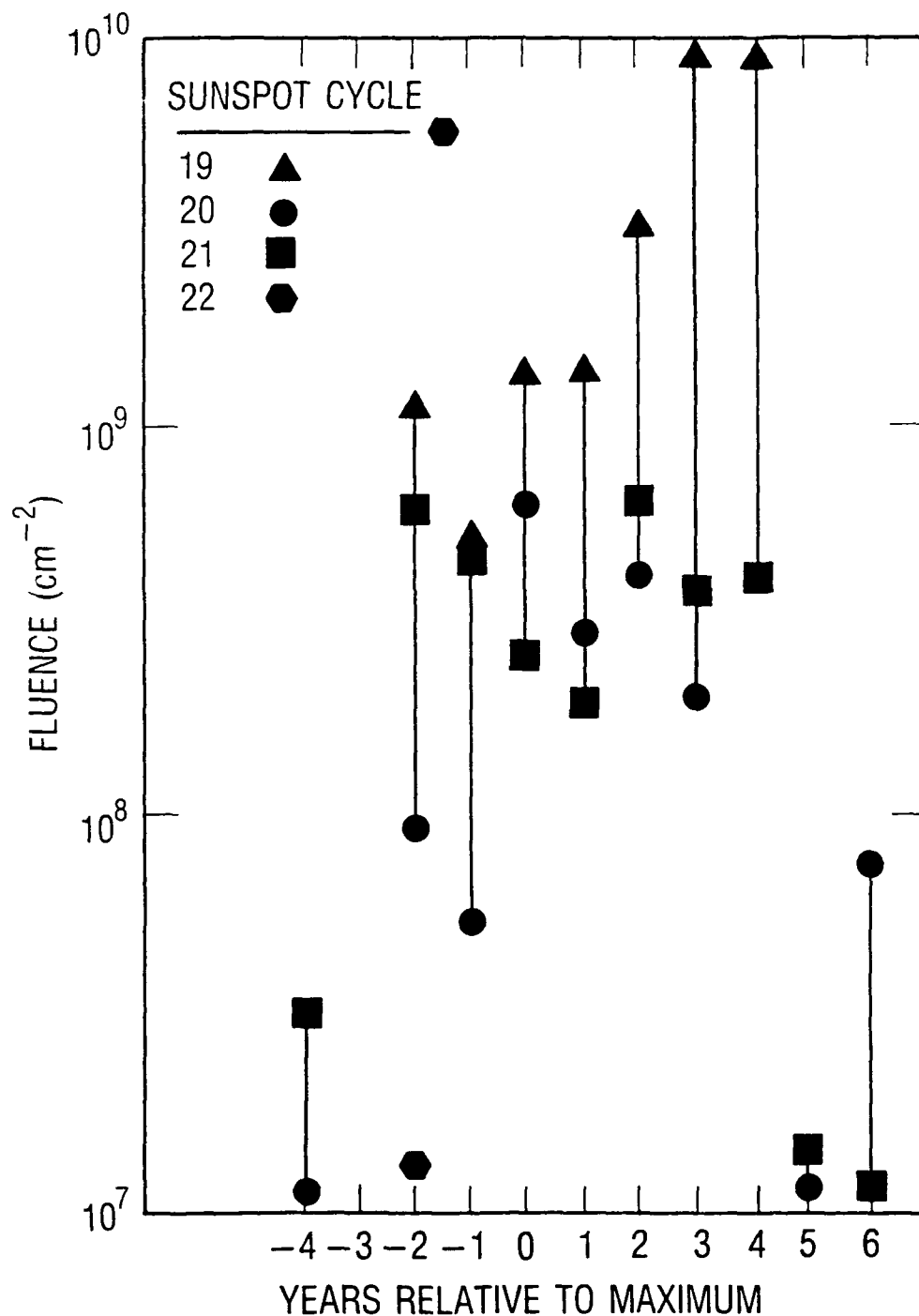


Figure 4. A Superimposed Epoch Representation of the Yearly Fluence of >30 MeV Solar Protons as a Function of Time Relative to the Year of Sunspot Maximum. Data are plotted for solar cycles 19 through 21 and for the first three years of solar cycle 22. Vertical lines through the data points indicate the complete range of values observed prior to cycle 22. The plot is from Zwickl and Kunches (1989) and Feynman and Gabriel (1990).

of expected fluence appropriate for short time intervals (see Feynman et al., 1988; Stassinopoulos, 1975; Chenette and Dietrich, 1984).

Some examples of the most severe proton events ever observed are shown in Figure 5. The plots show integral proton flux above 10 and 30 MeV, and where available above 100 MeV, for three ~ week-long periods. Note that two of the events are quite recent. These two were associated with solar cycle 22, and they occurred within one month of each other. For almost two decades prior to these recent events, however, the event of August 4, 1972 was regarded by many as representative of a "worst case", even though the originating flare was not optimally located on the sun for "direct connection" to the Earth. It was argued that the extreme magnitude of this event resulted from a unique sequence of events which was not likely to be repeated. This sequence of events involved the propagation of two (converging) magnetohydrodynamic shocks in interplanetary space at the time of the flare occurrence. The Earth was situated between these two shock structures during the time interval marked in Figure 5a. It is hypothesized (see Burlaga et al., 1987; Smart and Shea, 1989) that the solar proton population injected into the interplanetary medium interacted with these converging shocks and the particles trapped between the converging shocks underwent further acceleration via the Fermi process (see Lee, 1983, 1986), leading to the substantial (order-of-magnitude) increase in flux observed late on August 4, 1972.

It is interesting to note that the time profile and intensity of the event which occurred on October 19-20, 1989 is quite similar to that of the August 1972 event, although the association of the abrupt order-of-magnitude increase in flux in the 1989 event with converging interplanetary shocks has not been demonstrated clearly. The event on September 29, 1989 is included in this ensemble of examples because it represents the largest ground-level effect observed in over 30 years. The ground-level events observed in September and October 1989 caused several operational problems with spacecraft in deep space, both in geosynchronous orbit and in low-Earth orbit. These problems included enhanced background noise in star trackers, rapid degradation of solar arrays (up to five years equivalent

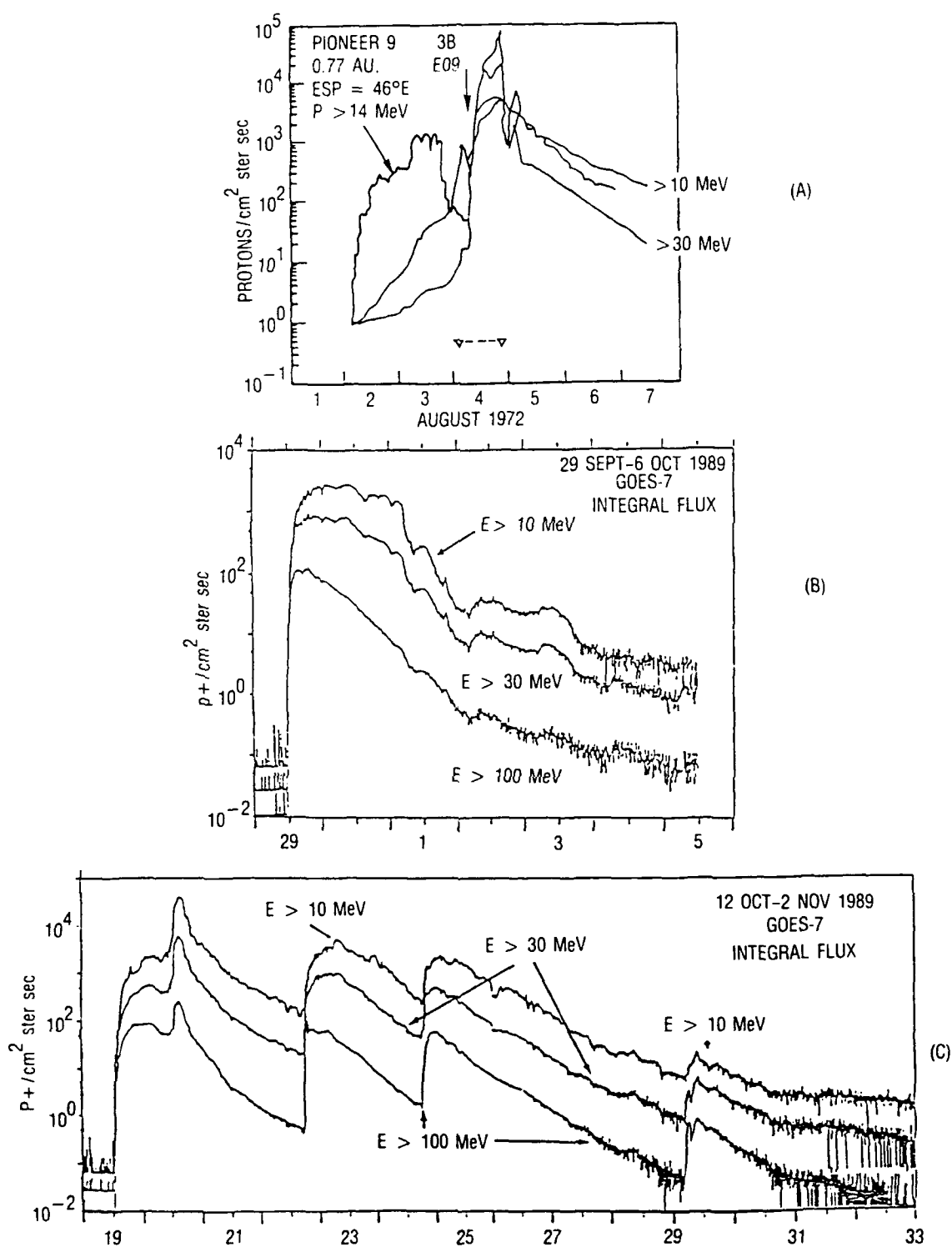


Figure 5. Examples of Three Intense Solar Proton Events Observed Over the Past Three Solar Cycles. Each plot shows several days of data surrounding the events. The plot of the August 1972 event is from Smart and Shea (1989), and the plots of the 1989 events are from Zwickl and Kunches (1989).

aging in less than one week), and numerous single-event upsets. Also, significant radiation levels were measured by dosimeters aboard transpolar airline flights at high altitudes.

Together, the three events shown in Figure 5 represent total proton fluences which exceed the sum of all other events which occurred during this 20-year time period. It is unlikely that any of these individual events represents a true worst case. Whether more events of this type are to occur in the remainder of cycle 22 is probabilistic, but historical evidence (e.g., Figure 4) indicates that several more significant events are likely to occur during the 1990-1995 time period.

2.2 GEOMAGNETIC ACTIVITY

While sunspots themselves have virtually no effect on geomagnetic activity, other solar parameters which do affect the terrestrial environment tend to be modulated along with sunspot numbers in an 11-year cycle. Also, the modulation amplitude of many other solar parameters tracks the sunspot number fairly closely (see Hirshberg, 1973). Thus, we might expect geomagnetic activity to be modulated at the 11-year sunspot cycle period by acquaintance (see Garrett et al., 1974; Mayaud, 1975). Figure 6 shows this to be the case. Figure 6 plots yearly averages of the sunspot number and an index of geomagnetic activity (Feynman, 1982, 1988) from 1870 to 1979, including data from solar cycles 11 through 21. The geomagnetic activity index shows a clear modulation corresponding to the 11-year sunspot cycle. However, the annual averages of geomagnetic activity do not maximize at the time of sunspot maximum (sunspot maxima are marked with arrows), nor do the cyclic peaks of geomagnetic activity correspond in magnitude to the amplitude of the nearest sunspot maximum. On closer inspection, the geomagnetic index tends to have a double-peaked modulation, with the major peak occurring during the declining phase (Gosling et al., 1977) of the sunspot cycle and a secondary peak occurring nearer to the sunspot maximum (Newton, 1948; Ohl, 1971). This double-peaked modulation is observed in the frequency of occurrence of major geomagnetic storms as well (see Allen, 1984; Walterscheid, 1989). The major peak is due to a tendency for strong solar

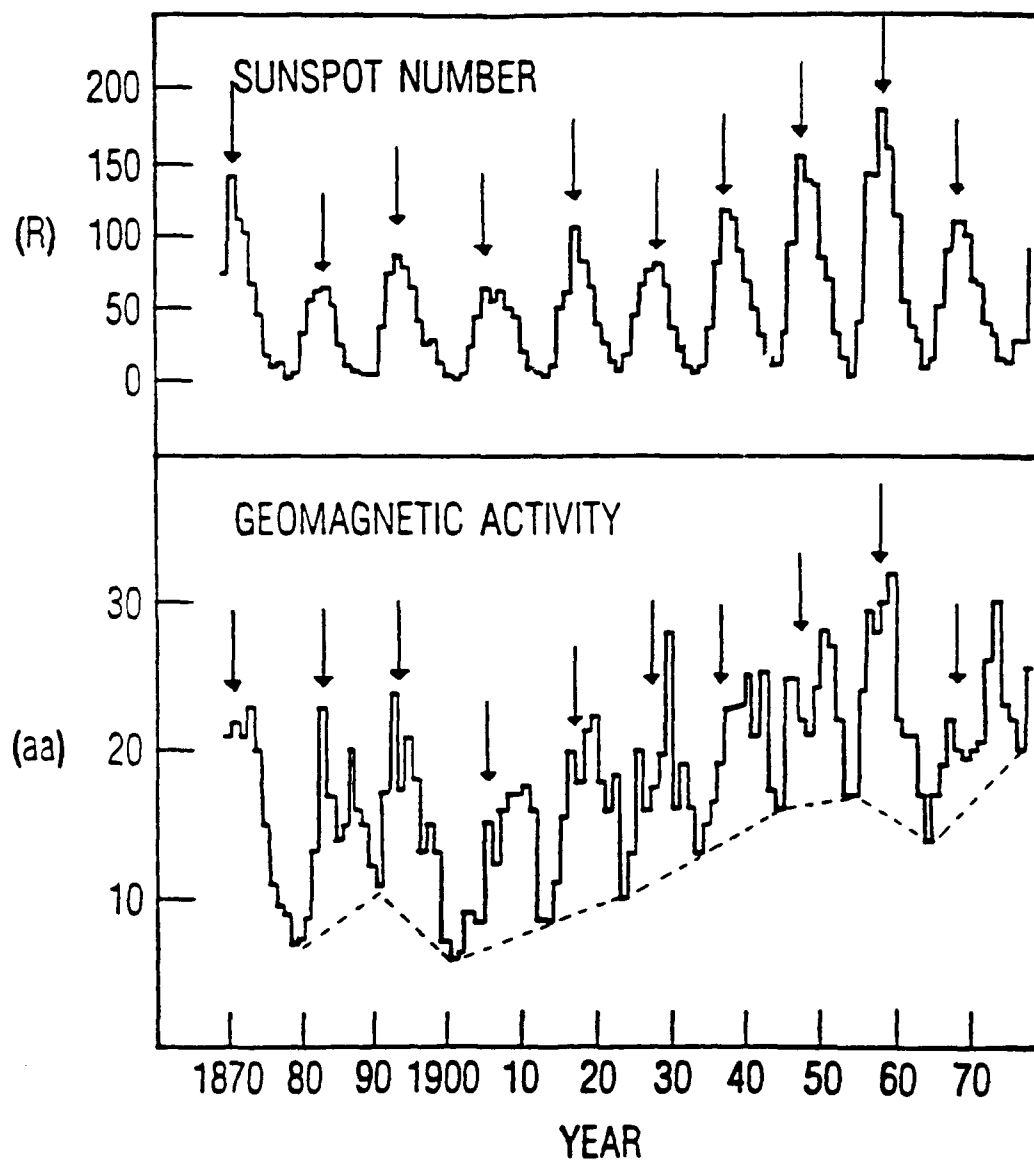


Figure 6. Annual Averages of Sunspot Number (R) and Geomagnetic Activity Index (aa) from 1870 to 1979. The data are from Feynman (1982, 1988).

wind streams to occur primarily during the sunspot declining phase. Both sunspots and coronal hole regions (coronal holes are regions of the solar atmosphere in which the magnetic topology is open to interplanetary space, thus allowing unrestricted outward flow of solar wind [see Hundhausen, 1972, 1977]) tend to occur at progressively lower solar latitudes as the sunspot cycle proceeds past its peak. Equatorial protrusions of coronal holes are a major source of strong solar wind streams in the ecliptic plane, which are known to cause enhanced geomagnetic activity (Neupert and Pizzo, 1974; Sheeley and Harvey, 1981).

The geomagnetic activity shows some evidence of a trend toward increasing magnitudes over the past several solar cycles (Feynman, 1982, 1980). The trend is especially apparent in the cyclic minimum values of the geomagnetic activity index, marked in Figure 6 with a dashed line. This feature has prompted some researchers to hypothesize a long-period (~80-year) cyclic behavior of solar wind parameters (Gleissberg, 1965). If this long-period modulation persists into the next solar cycle, we might expect somewhat higher average levels of geomagnetic activity even for relatively moderate values of sunspot numbers. As yet no firm physical basis has been identified for the longer-period behavior, and it would be risky to use the apparent trend for predictive purposes.

In light of the several recent predictions of enhanced sunspot activity for the upcoming maximum of solar cycle 22, it would be useful to have some concept for the overall relationship between the amplitude of the solar cycle and the magnitude of geomagnetic activity (if any relationship exists). Does a large sunspot number really mean enhanced geomagnetic activity? A relationship, of sorts, does exist. Figure 7 plots annual averages of geomagnetic activity (see Mayaud, 1980) versus annual sunspot numbers (Feynman, 1982). While the linear correlation between the two parameters is relatively poor, a clear relationship between the parameters is apparent nevertheless. Specifically, larger values of sunspot number seem to exclude the possibility of occurrence of low levels of geomagnetic activity. However, the highest values of geomagnetic activity do not necessarily occur during the years of highest sunspot numbers. The

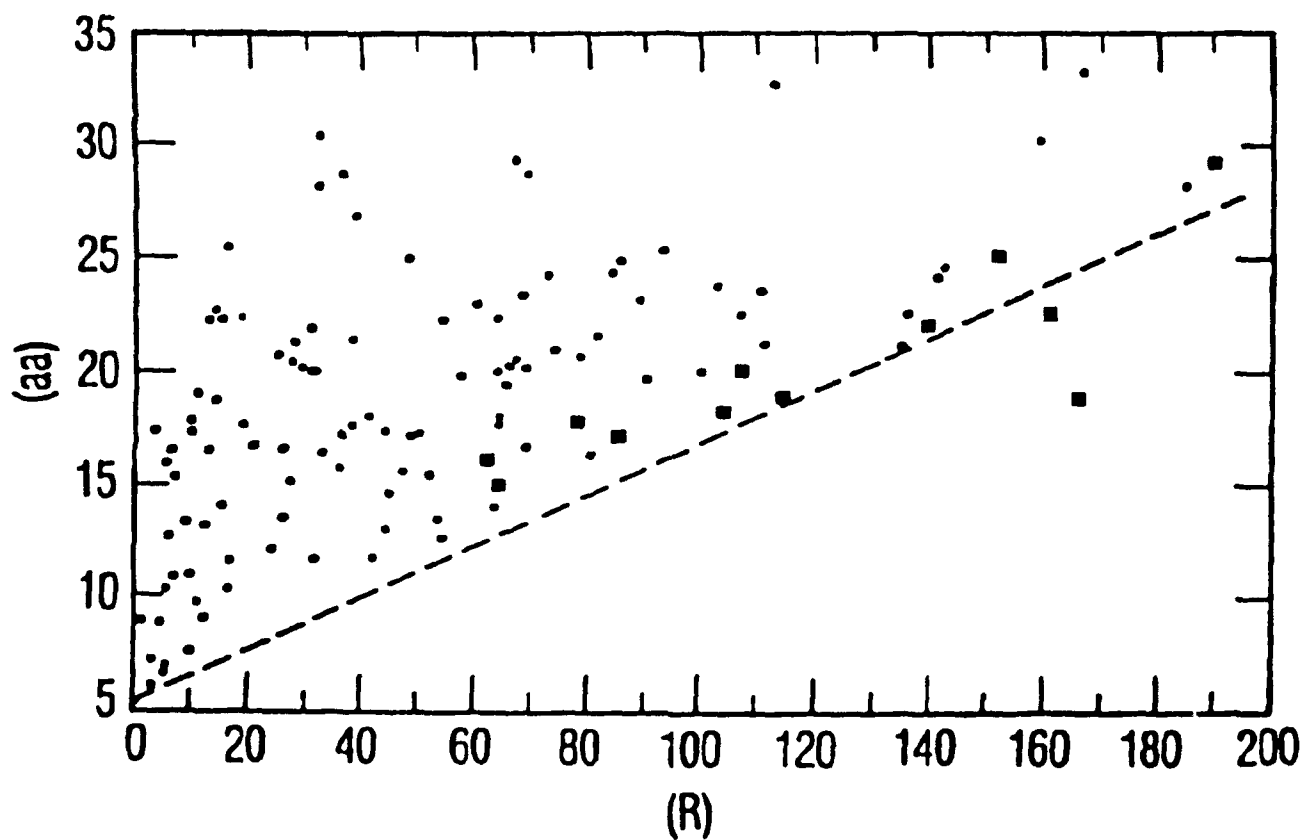


Figure 7. Annual Averages of the Geomagnetic Activity Index (aa) vs Sunspot Number (R). Data points corresponding to the individual years of solar cycle maxima are plotted with heavier points. The data are from Feynman (1982).

equation which represents the **minimum** activity for a given value of sunspot number is

$$aa_{(min)} = 0.12 R + 5.38 \quad (2)$$

This line represents the minimum activity for all but 2 out of 106 years of data. An interesting aspect of this relationship is that if the upcoming solar maximum is historically extreme (i.e., sunspot numbers in excess of 200 or so) then the average level of geomagnetic activity almost certainly will be historically extreme as well.

Data points corresponding to the individual years of solar cycle maxima are plotted with heavy squares in Figure 7. A curious feature of these particular data points is that they all lie very near the line of minimum geomagnetic activity. The implication is that solar activity is less effective in coupling to the terrestrial system during the solar maximum years than during the declining phase of the solar cycle. Again, this behavior is due to the tendency for strong solar wind streams to be spawned late in the solar cycle. If this relationship holds for solar cycle 22, the actual occurrence of an extreme solar maximum in 1990 or 1991 may be an excellent predictor of enhanced geomagnetic activity during the subsequent declining phase of the solar cycle.

Statistical results show a strong correlation between solar wind speed and geomagnetic activity. This relationship offers a reasonable explanation for many features of the correlation and phasing of the sunspot and geomagnetic activity cycles shown in Figure 6. Figure 8 shows histograms of the occurrence frequency distributions of solar wind speed over a period spanning a complete solar cycle (Gosling et al., 1976). The histograms are plotted yearly, from 1962 to 1974. The arrow on each plot shows the average speed for each year. Note that the average solar wind speeds are slightly enhanced in the solar maximum year 1968 and in the declining phase years 1962, 1973, and 1974. More importantly, note that the occurrence of extreme solar wind streams (speeds in excess of 700 km/sec) occur much more often in the declining phase years than in other phases of the solar cycle.

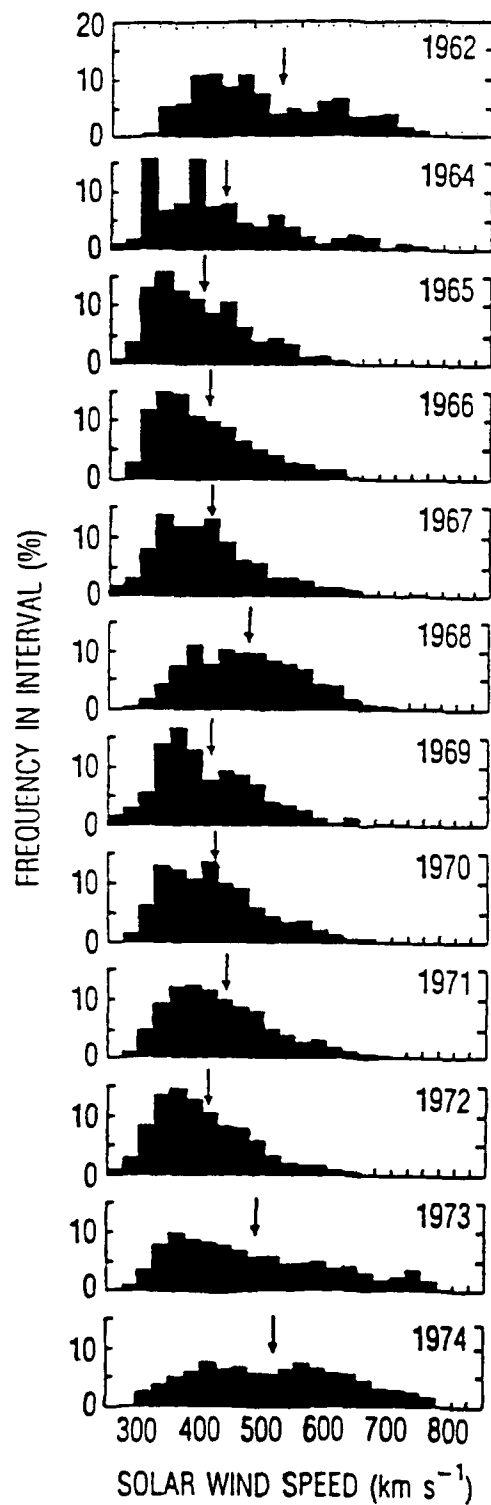


Figure 8. Histograms of Solar Wind Speed Distributions for the Years 1962-1974. Arrows indicate the yearly mean. Note that both the yearly mean speed and the occurrence frequency of very high speed streams show a significant dependence on phase relative to the solar maximum (~1969). The plot is from Gosling et al. (1976).

The occurrences of these extreme values of solar wind speed are correlated best with the highest levels of geomagnetic activity for this time period.

A great deal of observational evidence supports the hypothesis that the solar wind speed has a dominating influence on geomagnetic activity and related phenomena. Figure 9 shows stacked plots of six-month averages of the solar wind speed and of the global geomagnetic activity index ap (Gosling et al., 1976; Crooker et al., 1977). (The solar wind data are from the Mariner 2 data set (1962) and from the Vela and Imp spacecraft (1964-1975).) The ap index is a planetary magnetic activity index which has a roughly linear relationship to the magnitude of observed global geomagnetic deviations (see Mayaud, 1980). The correspondence between the two plotted quantities is clear. For long-term averages (-months) the ap index is found to correlate best with the **square** of the solar wind velocity, with a correlation coefficient greater than 0.8. (The correlation is so good that many researchers of historical solar data have been tempted to use geomagnetic activity indices as proxy data for solar activity measurements such as solar wind velocity (see Russell, 1975; Feynman and Silverman, 1980; Schröder, 1988; Silverman, 1983). On shorter time scales, which are more representative of the geomagnetic events themselves (minutes to hours), the correlation between solar wind speed and geomagnetic activity is much poorer. For these shorter time scales (see Baker et al., 1983, 1986), the magnitude and direction of the interplanetary magnetic field (IMF) appears to have a controlling influence on the level of geomagnetic activity. Specifically, the occurrence of sustained intervals of an IMF with a significant southward component is well correlated with the onset of geomagnetic storms. However, the IMF is very poorly correlated with geomagnetic activity over long time scales (the correlation coefficient between six-month averages of the southward IMF component and the ap index is less than 0.03 (see Crooker et al., 1977). It appears as though the overall envelope of geomagnetic activity is well correlated with the solar wind speed, while individual events may be "triggered" or at least modulated by the IMF. Other solar wind parameters, such as the plasma density and temporal variances of the speed and the IMF, have been found to

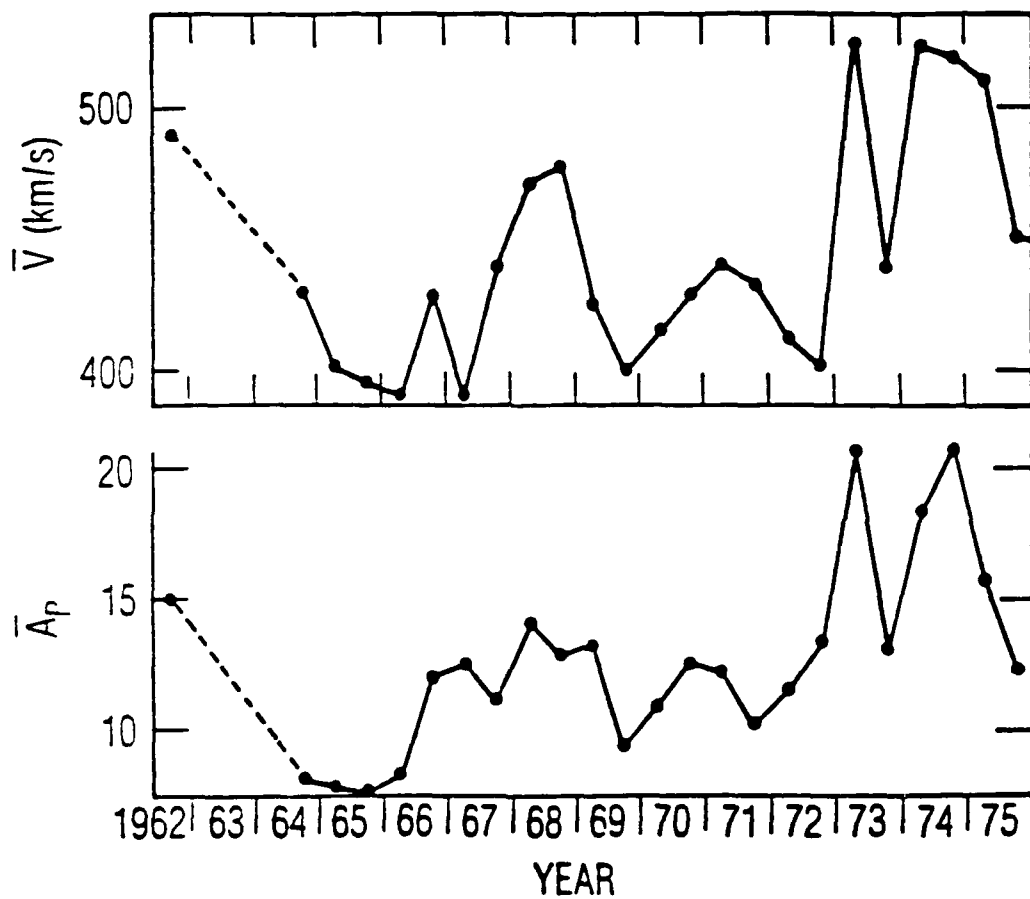


Figure 9. A Plot of Six-Month Averages of the Solar Wind Speed (V) and the Geomagnetic Activity Index (ap) for the Time Period Spanning 1962-1975 (see Gosling et al., 1976; Crooker et al., 1977).

correlate with the level of geomagnetic activity as well. Recently, Gonzalez et al., (1989) studied solar wind - magnetosphere coupling during very intense magnetic storms and showed that a small set of functional forms involving solar wind speed, density, pressure, and IMF could be used to obtain excellent correlation with geomagnetic activity as measured by the geomagnetic index D_{st} . Table 1 summarizes a group of published empirical and theoretical relationships between solar wind parameters and various measures of geomagnetic activity (compiled from Crooker et al., 1977; Snyder et al., 1963; Olbert, 1960; Garrett et al., 1974; Maezawa, 1979; Murayama, 1979; Feynman and Crooker, 1978; Burton et al., 1975).

Table 1. Empirical and Theoretical Relationships Between Geomagnetic Activity and Solar Wind Parameters.

Source reference	Geomagnetic Activity Index	Functional Relationship to Solar Wind Parameter(s)
Snyder et al. (1963)	ΣK_p	$\Sigma K_p = (V-330)/8.44$
Olbert (1960)	ΣK_p	$\Sigma K_p = (V-262)/6.30$
Garrett et al. (1974)	a_p, AE	$a_p, AE = C_1 + C_2 V B_z + C_3 V^2$
Murayama (1979)	AE	$AE = C B_z V^2$
Burton et al. (1975)	D_{st}	$dD_{st}/dt = F(V B_z) - C_1 D_{st}$
Crooker et al. (1977)	a_p	$a_p = 3.5 \times 10^{-5} B_z V^2 - 1.9$
	a_p	$a_p = 7.0 \times 10^{-5} V^2 - 1.8$
Feynman and Crooker (1978)	aa	$aa = 1.3 + 4.7 \times 10^{-5} B_z V^2$
Maezawa (1979)	AL	$AL = B^{0.85} V^{2.08} (\sin \theta)^{0.54}$
	AU	$AU = B^{0.67} V^{1.15} (\sin \theta)^{0.34}$
	am	$am = B^{1.03} V^{2.34} (\sin \theta)^{0.37} n^{0.2}$
Murayama (1979)	AL	$AL = 60(B_z + 0.5)V^2 n^{0.13} F(B_y)$
Gonzalez et al. (1989)	D_{st}, ϵ	$\epsilon = 3 \times 10^{20} (d/dt + 1/\tau) D$

Functional relationships between solar wind and geomagnetic parameters provide important information on the processes which couple energy between the two systems. The relationships are also useful for scaling the effects of anticipated enhancements in solar activity in terms of geophysical effects. However, for practical purposes it would be more useful to be able to predict the expected number and severity of individual geomagnetic "events" than to have a clear understanding of how average quantities might vary from year to year (see Feynman and Gu, 1986). As is the case for many interactions between man and nature, the occasional occurrence of extreme conditions (hurricanes, tornados, volcanic eruptions, earthquakes, etc.) can be more critical than longer-term variations. Unfortunately, the complexity of solar-terrestrial interactions makes it difficult to predict events or even to compile usable statistical information on geomagnetic events.

One major part of the problem of studying geomagnetic activity in terms of "events" is depicted in Figure 10, which shows several hypothetical representations of the coupling of energy between the solar wind and the terrestrial system (Akasofu, 1981). If the interaction were a purely driven process, the solar wind energy (ϵ) would couple directly into the magnetosphere and be dissipated (U), perhaps with some characteristic time delay (τ). The time series of energy dissipation (a combination of particle energization, joule heating of the atmosphere, auroral activity, and other processes which affect man-made systems) would be correlated well with the solar forcing and the terrestrial effects would be easy to predict. In an unloading or triggered process, the solar wind energy first would be stored, then released at some later time, possibly by an independent triggering mechanism. In an unloading system, the onset, magnitude, and duration of a geomagnetic "event" need not be well correlated with the forcing. Event prediction would require complete knowledge of the energy coupling process, the storage mechanism, and the triggering mechanism. In reality, the terrestrial system exhibits characteristics of both a driven and a triggered system. Even worse, some individual events exhibit a mostly driven character, while others respond as an unloading system.

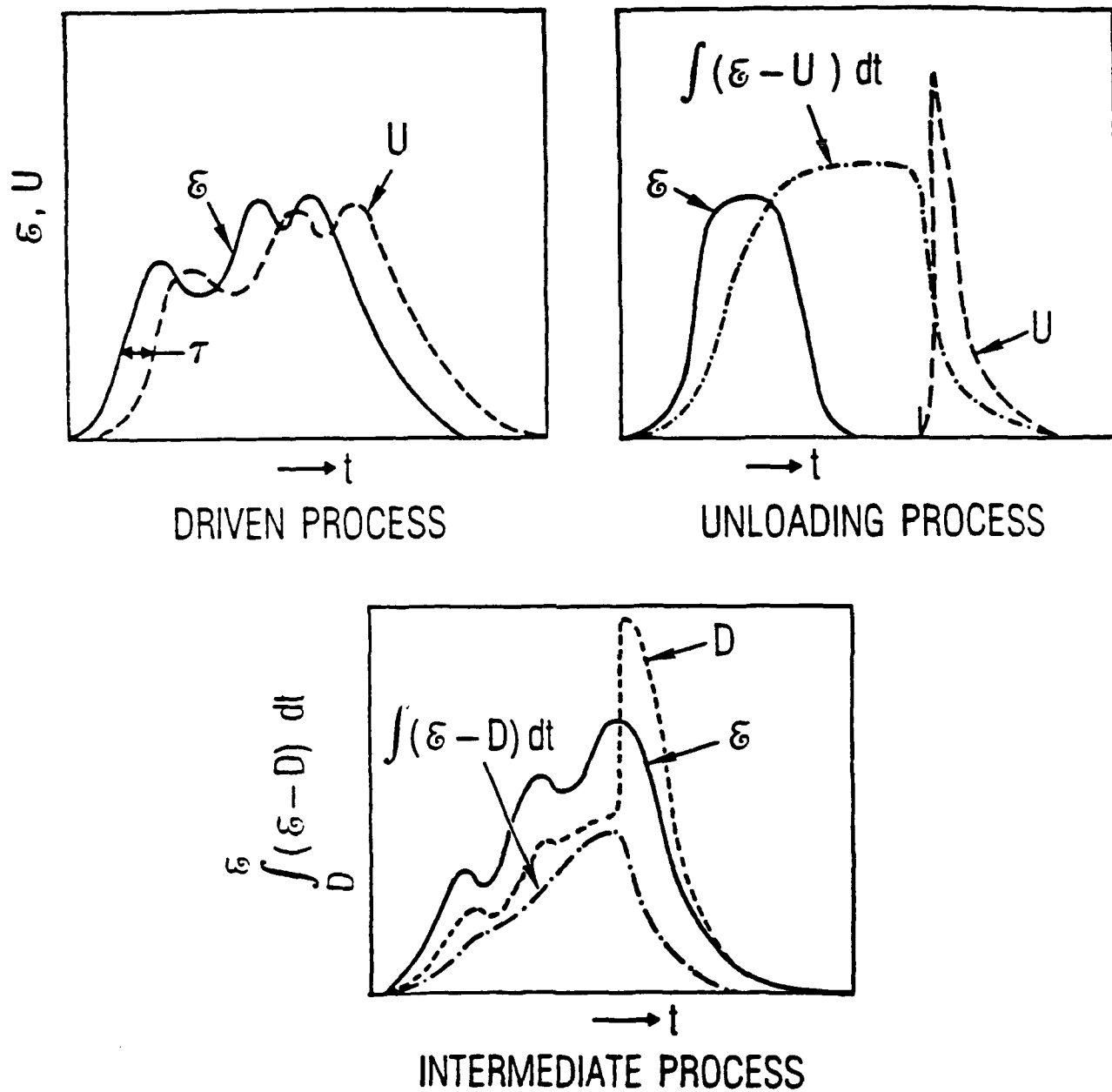


Figure 10. Examples of Energy Coupling in a Purely Driven System, a Purely Triggered System, and a Complex System (from Akasofu, 1989). In these diagrams, the quantity ϵ represents the energy incident on the magnetosphere while U and D represent profiles of energy dissipation within the magnetosphere.

Thus, it is difficult to predict which solar events will cause the most extreme geomagnetic conditions. Also, this complex coupling behavior can lead to difficulty in interpreting statistical correlations. In particular, some parameters which correlate on short time scales may not correlate well for long-term averages, and parameters which correlate in a long-term average may not be good predictors of individual events. We have seen some evidence of this effect in the statistical correlations between solar wind velocity or the IMF with geomagnetic activity, and in the variety and occasional disparity between the parametric relationships listed in Table 1. It is important to recognize that the formulations listed in Table 1 apply only on time scales characteristic of the averaging period for the individual activity indices, and that none of the formulations offer a true predictive capability for extreme events.

The observed correlations between solar activity and geomagnetic activity imply that many communications and space systems could be adversely affected during an extreme solar maximum and for several years thereafter. It should be noted that the cited correlations have utilized indices of geomagnetic activity. Measurements of the solar cycle dependences of actual plasma parameters (i.e., plasma temperature, density, composition) are rare and difficult to accomplish (see Yau et al., 1985; Collin et al., 1987 as examples). This difficulty arises from the finite lifetimes of experimental satellites (typically much less than 10 years) and from uncertainties in cross-calibration of instruments on different satellites. In the case of magnetospheric plasmas, an index of geomagnetic activity may be the most practical indicator of the expected environmental effects.

Although it is difficult to utilize the present state of empirical knowledge of solar wind-magnetosphere coupling for long-term predictions, historical evidence implies that the ever-increasing levels of solar activity in solar cycle 22 should lead to consequential geomagnetic activity. Indeed, the geomagnetic storm of March 12-14, 1989 (see Allen et al., 1989) provides at least anecdotal evidence of the relationship between high levels of solar activity and the occurrence of extreme geomagnetic events.

The March 1989 geomagnetic storm was preceded by a series of very intense solar flares on March 5, 9, and 10. A solar proton event commenced on March 7 and then decayed gradually over the next few days. A great geomagnetic storm was prefaced with a storm sudden commencement (SSC) on March 13, and geomagnetic activity remained extremely high for several days. During this storm, record levels of geomagnetic activity were observed. For example, the 24-hour aa magnetic activity index reached a value of 450, the largest 24-hour value recorded since this activity index began being documented in 1868. The 24-hour ap index (a more comprehensive index, documented since 1932) was 312, the third highest on record. During this storm, the aurora was visible well equatorward of 40° geomagnetic latitude, and red aurora were reported at latitudes as low as the Gulf of Mexico and Cancun, Mexico. Magnetic deflections exceeding 2000 nT were observed at mid-latitudes, and compass deviations of several degrees occurred at middle and high latitudes. Also affected was a wide variety of communication, navigation, and direction-finding systems, including the LORAN system. A power failure in eastern Canada, caused by the effects of enhanced ionospheric currents during the storm, affected some 6 million customers for over nine hours. Regardless of whether sunspot numbers for cycle 22 exceed previous record values, the geomagnetic activity and solar particle events of 1989 already place this cycle amongst the most extreme in terms of recorded effects on the near-Earth environment.

2.3 THE NEUTRAL ATMOSPHERE

Solar activity affects the Earth's neutral atmosphere at virtually all altitudes. Ground-level effects, including subtle variations in weather patterns and climatic changes, are thought to be related to solar output over the long term (see Eddy, 1977, 1978). Generally, the mechanisms which have been proposed for accomplishing the "sun-weather" relationship fall into the following categories: (a) variations in the terrestrial heat budget due to changes in the solar constant, (b) variations in the terrestrial heat budget due to minor modifications in the chemistry of middle-atmospheric constituents which are important in radiative and dynamic processes, and (c) effects on weather patterns due to changes in the fair-

weather electric field influenced by magnetospheric and ionospheric processes. These effects are not described in further detail here. The reader is directed to the reviews by Eddy and the references therein for further details on the topic of sun-weather relationships.

As one might expect, variations in the neutral atmosphere are more dramatic and occur on shorter time scales with increasing atmospheric altitudes. Indeed, order-of-magnitude variations in the neutral atmosphere density can occur at altitudes (~150-1000 km) where low-Earth-orbiting satellites fly (see Walterscheid, 1989). These effects have significant operational consequences for satellites flying through these low altitude regions, on space vehicles re-entering the atmosphere, and on systems which must track and monitor satellites and space debris. Although variations in total density are most important operationally, variations in composition, particularly variations in highly reactive constituents such as atomic oxygen (see Walterscheid, 1989), can have important impacts on the survivability and operation of space systems as well. Although solar cycle variation in atomic oxygen is not significant at altitudes below about 200 km, the atomic oxygen concentration at higher altitudes (500-800 km) can vary over the solar cycle by as much as a factor of 1000. High concentrations of atomic oxygen can react chemically with various surfaces of a satellite or sensor, leading to mass loss from external structures and degraded sensor performance (see Visentine, 1988).

By far the most dominant aspect of solar variability which leads to modulation of upper atmospheric parameters, is the sun's output of radiation in the extreme ultraviolet (EUV) wavelength band. All of the solar EUV flux which is incident on the Earth's atmosphere is absorbed within the thermosphere, and about 20-30% of the absorbed energy contributes to bulk heating of the thermosphere (Torr et al., 1980). Over the 11-year solar activity cycle, solar EUV emission varies by about a factor of 2 in integrated intensity (compared to <0.2% variability in the light output in the visible portion of the spectrum), and this variation in irradiance can cause substantial solar-cycle variations in the composition, temperature, density, and wind distribution of the Earth's thermosphere. Since solar

EUV radiation is absorbed entirely within the Earth's upper atmosphere, measurements of the solar EUV output must be performed in space, using either rocket- or satellite-borne sensors. Therefore, long-term (i.e., historical) data on variability of solar EUV do not exist (however, see Hall et al. 1985; Killeen, 1987; Schmidtke, 1984; Hedin, (1984); Donnelly, 1987; and Roble, 1987; for overviews of recent results). In particular, the continuity of the data is not sufficient to firmly establish the amplitude of solar EUV variability of an entire 11-year solar cycle (see Hirman et al., 1988). However, the existing data are sufficient to demonstrate clear temporal trends in solar EUV output and clear relationships between solar EUV flux and other measures of solar activity such as sunspot number and solar radio flux (see Hinteregger, 1980). The 10.7 cm solar radio flux index ($F_{10.7}$) correlates particularly well with solar EUV output, and the $F_{10.7}$ index is often used as a proxy index to characterize the solar EUV flux for computation of atmospheric effects (Walterscheid, 1989).

Enhanced geomagnetic activity, which is correlated with solar activity, is another (though secondary) mechanism by which the upper atmosphere is influenced by variations in solar activity. Geomagnetic effects on the Earth's upper atmosphere tend to be isolated to the high-latitude regions and tend to be more sporadic and episodic than the global effects of long-term variability in EUV output. The principal effect of geomagnetic activity on the neutral atmosphere is one of intense localized warming of the atmosphere in the polar and auroral regions. This warming is caused by two processes: (a) kinetic heating caused by the precipitation of energetic charged particles and (b) joule heating caused by enhanced ionospheric currents in the auroral zone. Typically, the joule heating rate exceeds the effects of direct particle precipitation by a factor of 3 to 10 (Ahn et al., 1989).

The primary operational effect of variability of the upper atmosphere is the effect of neutral density on satellite drag. Short-term variations in density, such as those which occur during geomagnetic events, perturb the orbital motions of satellites, leading to difficulties in tracking and

cataloging of objects at low altitude. These short-term perturbations also can lead to uncertainties in position for re-entering or sub-orbital vehicles. Long-term variations in atmospheric density, such as those driven by solar-cycle variations in EUV irradiance, have order-of-magnitude effects on satellite lifetimes in low-Earth orbit. Figure 11 shows satellite lifetimes as a function of the $F_{10.7}$ solar index for circular orbits of various initial altitudes (from Walterscheid, 1989). The plot is constructed for a relatively small vehicle of low cross section (typical of Explorer-class vehicles) and shows a range of indices characteristic of the extremes of solar minimum and maximum. Note that the lifetime of a satellite at an initial altitude of 500 km during quiet solar conditions is about 30 years, whereas the lifetime of the vehicle is limited to just over 2 years during active solar conditions. Since 30 years is much longer than the ~11-year solar activity cycle, and 2 years is much shorter than the solar cycle, the actual lifetime of such a vehicle clearly would be limited by the duration and intensity of the solar activity during the solar maximum time period.

2.4 THE IONOSPHERE

The Earth's ionosphere is a relatively thin layer of partially-ionized magnetized plasma extending from ~80 km to ~500 km altitude. Typical plasma densities in the ionosphere (see Jasperse, 1981) range from 10^3 - 10^6 cm^{-3} , compared with neutral densities of about 10^7 - 10^{16} cm^{-3} . Because of the strong coupling between the ionosphere and the sun, and the atmosphere and the magnetosphere, the phenomenology of the ionosphere is complex and has been under scientific examination for many years. In order to categorize the various physical processes which govern ionospheric structure, one must subdivide the ionosphere into at least two or three layers in altitude, two or three zones in latitude, and consider the day and night ionosphere separately. No attempt will be made here to review all the fundamentals of ionospheric physics for each of these regions, but it is necessary to point out some of the key relationships between solar activity and ionospheric structure.

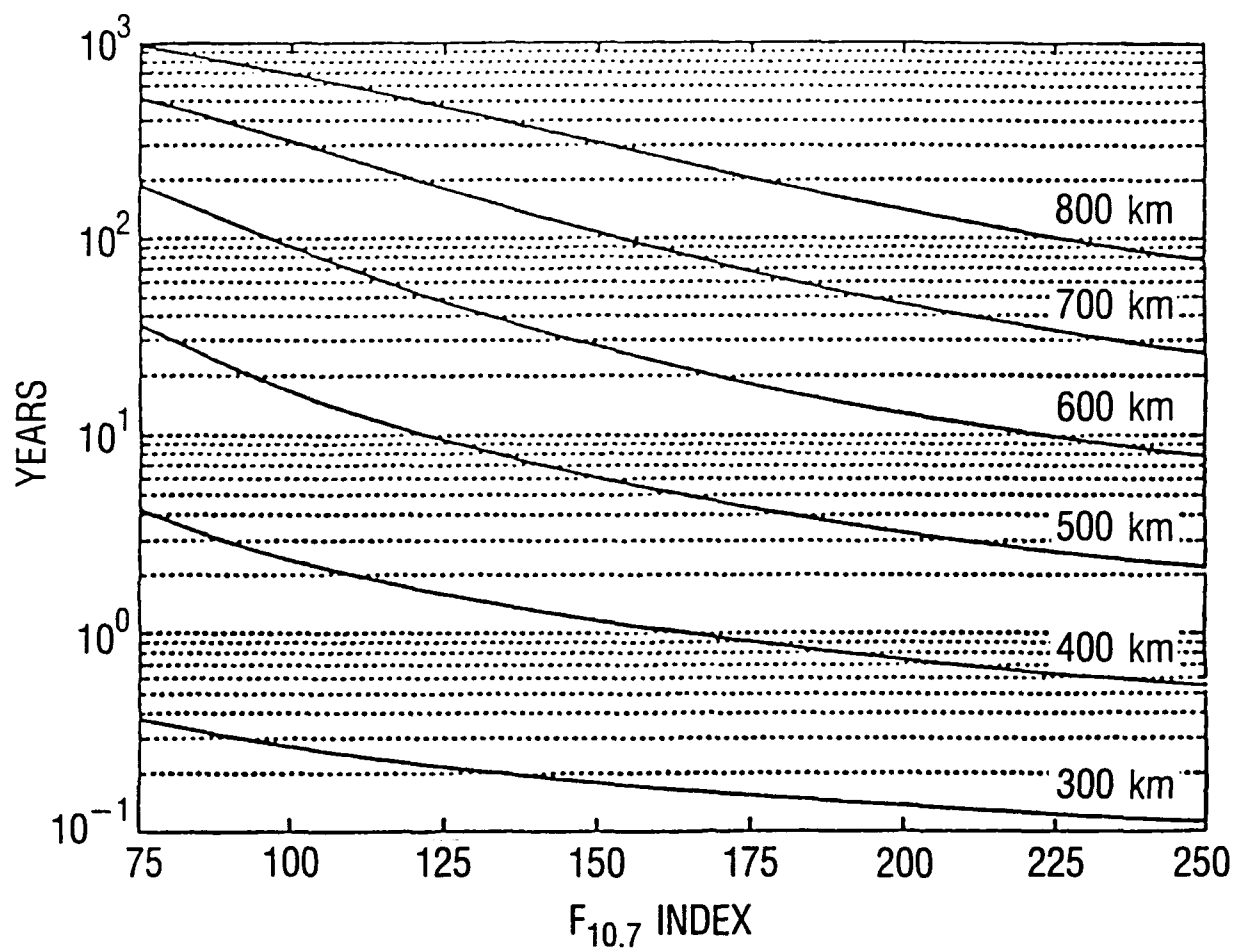


Figure 11. A Plot of Satellite Lifetimes vs Solar 10.7 cm Radio Flux ($F_{10.7}$) for Several Initial Altitudes, from 300 km to 800 km. The plot is constructed for a small vehicle with modest cross section, such as an Explorer-class spacecraft (the plot is from Walterscheid, 1989).

By far the most important subdivision of the ionosphere, especially at equatorial and midlatitudes, is that between day and night. During the day, the most important ionizing agent is direct solar illumination at ultraviolet (UV) wavelengths, which contributes an average ionizing energy flux of about $5 \text{ ergs/cm}^2\text{sec}$. Photoionization balances collisional recombination in the E (90-120 km altitude) and F (~250 km) regions of the ionosphere, with peak steady-state ionization densities occurring in the 250-400 km altitude range. The peak ionization density and the column total electron content (TEC) of the ionosphere responds directly and abruptly to variations in the solar UV radiation, and several 10s of percent changes in these quantities can occur essentially without warning during severe solar flare conditions (Mendillo et al., 1974). Ultimately, the peak ionization density controls the maximum radio frequency that can execute multiple-hop raypaths, and TEC affects frequency management and range corrections for transionospheric communications, tracking, and navigational signals. The critical transmission frequencies of the ionosphere, corresponding to peak ionization densities in the E and F regions, are called the f_oE and f_oF_2 frequencies. These frequencies can vary from 1-3 MHz in quiet solar conditions to >15 MHz in very active conditions. Navigational range errors caused by the effects of TEC variations on space-based radio beacon transmissions are usually small, but can be important for the most critical applications. At night the solar-induced ionization densities collapse rapidly (in seconds at low altitudes and in a few hours at higher altitudes). This rapid collapse, along with dynamic effects near the dusk terminator, lead to the development of ionization plumes and irregularities which also affect radio-frequency propagation in the dusk-midnight local time sector (Basu et al., 1988).

The D region of the ionosphere, at about 80 km altitude, also experiences abrupt and direct effects of solar activity. Solar flare x rays and relativistic protons arrive at the Earth within minutes of the occurrence of a solar flare. This radiation can penetrate into the ionospheric D region and momentarily can become the dominant ionization source there. The solar flare protons generally gain access to the Earth at high

latitudes only, but can cause measurable increases in D region ionization. These effects can be observed as increases in the absorption of cosmic radio noise, and the occurrences are called polar cap absorption (PCA) events. At times, fluxes of relativistic electrons from interplanetary space can have significant effects on the ionospheric D region. While the source of the relativistic electrons is not understood thoroughly, the events do show a dependence on the solar cycle (see Baker et al., 1987). The D region events can cause disruption of short-wave and airline communications, and can have deleterious effects on other reconnaissance systems.

At high latitudes, the precipitation of energetic ions and electrons from the magnetosphere and ionosphere (the same particles which are responsible for stimulating the visible-light emissions in auroral displays) is the dominant ionization source. The magnitude of the precipitating particle flux varies enormously, from less than one to several hundred $\text{erg/cm}^2\text{sec}$. The magnitude of the precipitation is correlated directly with the occurrence of geomagnetic events which can last from several minutes to several days. During these events, ionospheric parameters such as $f^\circ E$, $f^\circ F2$, and TEC can vary dramatically and can develop strong horizontal gradients. The auroral zone is also the primary location for the development of small-scale time-varying regions of ionization which can cause severe phase and amplitude scintillations (i.e., fades) at HF, VHF, and UHF frequencies.

During auroral events, strong electrical currents flow through the high-conductance channels in the ionosphere caused by localized ionization enhancements. These regions experience resistive or joule heating which can have consequences for the energy balance of the neutral atmosphere (global joule dissipation rates as high as a terawatt are possible). As a result of enhanced joule heating, "bulges" can develop in the neutral atmosphere above ~ 100 km, affecting the trajectories of low-flying and re-entering satellites (along-track location errors of several kilometers can occur in periods of hours). The ionospheric current systems (known as "electrojets") cause other observable effects, including the induction of

electrical currents in large man-made conductors such as oil pipelines, telegraph or telephone lines, and power distribution grids.

Comprehensive data sets and relatively rigorous theoretical treatments have been developed for ionospheric effects. Typically, solar-illumination effects on the ionosphere tend to be direct effects which are relatively easy to quantify. For example, some ionospheric-critical frequencies are known to respond to variations in solar activity with the following (approximate) dependence (Davies, 1965):

$$f_oF_2 \text{ (MHz)} = (4.3 + 0.01 R) (\cos \chi)^b \quad (3)$$

where χ is the solar zenith angle and $b \sim 0.5$. The linear dependence on sunspot number, R , implies important consequences of an enhanced (e.g., $R \sim 200$) solar maximum. Indeed, the effects of enhanced solar UV and EUV radiation on the ionosphere could be the most global and most prolonged effects of the solar cycle on the terrestrial system.

The ionospheric effects on communication links have been studied for extended periods of time with a large variety of measurement techniques. Some of the most effective measurement techniques are the communications systems themselves, from which qualitative but useful data on ionospheric "weather" conditions can be acquired globally. Indeed, skilled short-wave radio operators can sense, analyze, correct for, and even utilize changing ionospheric conditions in near real time. More quantitative ionospheric sensing over the past several decades has included riometry, backscatter radar, ionosondes, *in situ* measurements from rockets and satellites, topside ionospheric sounders, multi-wavelength ionospheric imagery, and ground-satellite radio beacon measurements. Each of these sensing techniques has contributed immense data sets over the years on both the large-scale and small-scale ionospheric responses to changing solar and geomagnetic conditions. Much of these data and related theoretical formulations have been incorporated in numerical (parameterized) ionospheric specification models for operational applications. Some specific examples of parameterized relationships between solar or geomagnetic activity indices and

indices and ionospheric parameters are listed in Table 2 (compiled from Tascione et al., 1988; Lloyd et al., 1978; Elkins and Rush, 1973; Wakai, 1967; Gassman, 1973; Vondrak et al., 1978; Wagner, 1972). Note the relatively independent nature of the global (mid-latitude) and auroral (high latitude) ionospheric effects.

Table 2. Empirical Relationships Between Solar-Geomagnetic Activity Indices and Ionospheric Parameters.

Source Reference	Ionospheric Parameter (Units)	Functional Relationship
Davies (1965)	f_oF_1 (MHz)	$f_oF_1 = (4.3 + 0.01R)(\cos \chi)^b$ $b = 0.2 + 0.3(\chi - 90)/15.5$
Lloyd et al. (1978)	hmF_1 (km)	$hmF_1 = 165 + 0.642\chi$
Elkins and Rush (1973)	f_oE_{solar} (MHz)	$f_oE_s = A(\cos \chi)^m(1 - .0038(12-T) - .00013ap)$ $m = 0.25$
Elkins and Rush (1973)	hmE (km)	$hmE = 100 + 20 \ln(90x_E)$ $x_E = \chi(90/101) \quad (\chi < 76.78^\circ)$
Wakai (1967)	hmE (km)	$hmE = 120 \quad (\chi > 76.78^\circ)$
Gassman (1973) and Vondrak et al. (1978)	$f_oE_{auroral}$ (MHz)	$f_oE_a = 2.5 + Q_E/9 \quad 0 < Q_E < 2.7$ $f_oE_a = -1.0 + 7Q_E/5 \quad 2.7 < Q_E < 4.2$ $f_oE_a = 3.2 + 2Q_E/5 \quad Q_E > 4.2$
Gassman (1973) and Vondrak et al. (1978)	hmE_a (km)	$hmE_a = 185 \quad f_oE_a < 2$ $hmE_a = 185 - 30(f_oE_a - 2) \quad 2 < f_oE_a < 3.5$ $hmE_a = 145 - 10(f_oE_a - 3) \quad 3.5 < f_oE_a < 9$
Wagner (1972)	f_oE (km)	$f_oE = (1.5(f_oE_a)^4 + (f_oE_s)^4)^{1/4}$

In addition to the direct variations of ionospheric parameters caused by solar or geomagnetic activity, the formation of small-scale ionization irregularities can cause severe impacts on VHF/UHF communications links (Basu et al., 1988). Time-varying, small-scale (<1 km) irregularities can cause amplitude and phase scintillation of transionospheric radio links and tracking radar signals at VHF through UHF frequencies. The effects of ionization irregularities on transionospheric radio links has been studied directly over the past several years through the use of space-based radio beacons in low polar and geostationary orbits, and on the Global Positioning System (GPS) satellites. By positioning ground-based receivers at several sites world-wide, and by operating the receivers continuously over several years, comprehensive data of the effects of solar and geomagnetic activity on the formation of ionospheric irregularities and on the occurrence of signal fades has been acquired. Figure 12 shows an example of a long-term data set acquired from a VHF (250 MHz) receiver at Thule, Greenland (Basu et al., 1988). The plot shows the monthly-average occurrence frequency of signal fades at four different levels (>5 dB, >10 dB, >15 dB, and >20 dB) over the 1979-1986 time period, spanning the solar-cycle 21 maximum and subsequent minimum. A clear correlation between the frequency and severity of signal fades with sunspot number is evident. Note that severe (>20 dB) signal fades can occur as much as 50% of the time during solar maximum (weak fades occur as much as 90% of the time), while even weak (5 dB) fades occur less than 5% of the time during solar minimum years. At high latitudes, seasonal modulation is as important as any other factor in determining fade occurrence frequency. Kilometer-scale irregularities do not tend to occur during the local summer solstice at high latitudes. Figure 12 shows that extreme solar activity levels certainly would be accompanied by high frequencies of severe VHF fades at high latitudes. On the other hand, signal fades (at VHF and UHF) are a relatively common and important problem even during modest solar activity.

Figure 13 summarizes the global occurrence characteristics of L-band (1-2 GHz) fades (Basu et al., 1988) for both solar maximum and minimum periods (with some extrapolation of VHF results). Three regions of

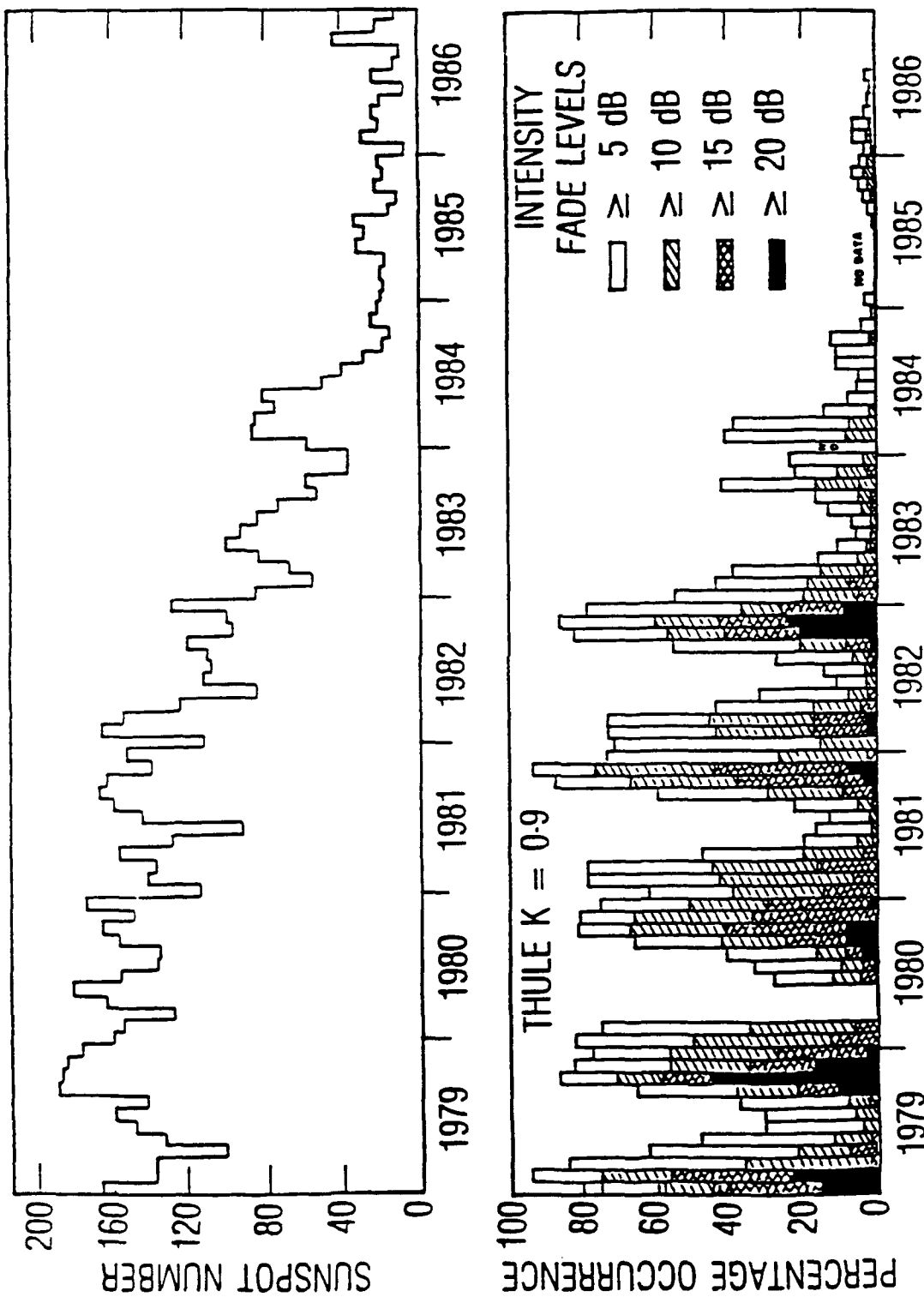


Figure 12. Histograms of the Occurrence Frequency of Signal Fades at Thule, Greenland Compared to Monthly-Average Sunspot Number from 1979 to 1986 (from Basu et al., 1988).

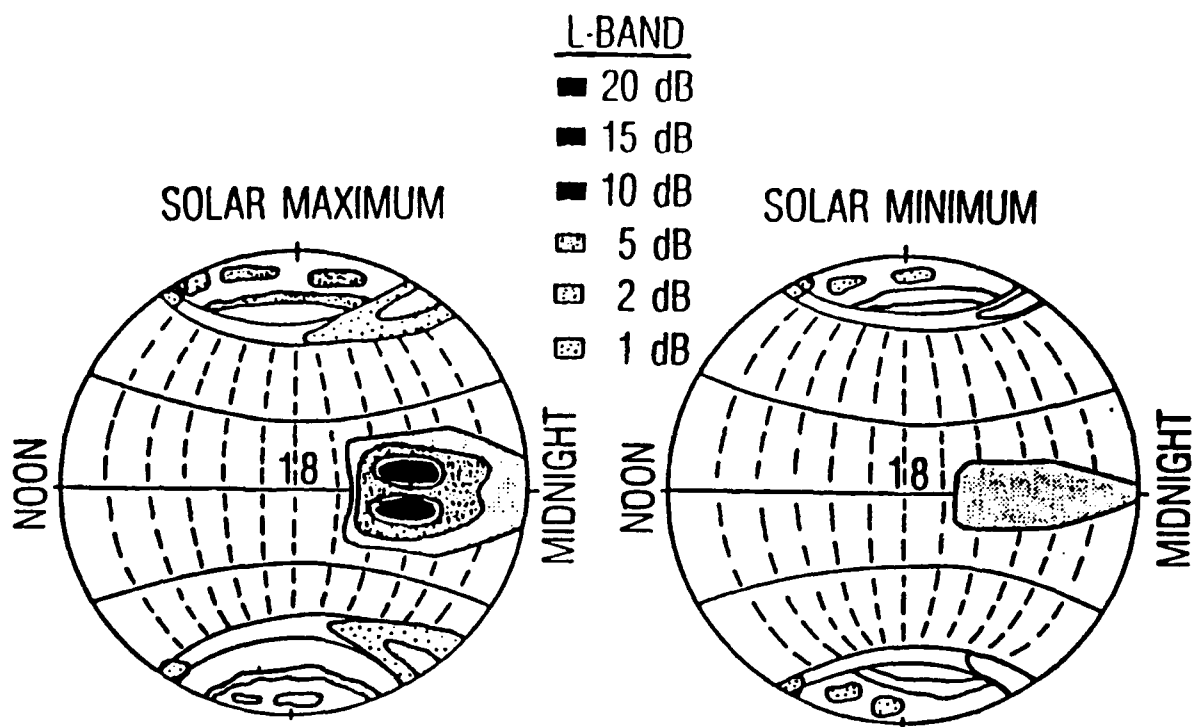


Figure 13. Local-Time-Latitude Plots of the Regions and Severity of Signal Fades During Solar Maximum and Minimum Periods (from Basu et al., 1988).

ionospheric scintillation are identified: the equatorial region in the post-sunset local time period, the auroral band, and the polar cap region. The most disturbed areas occur on either side of the equator. Scintillation effects maximize where the local magnetic dip angle is about 30° , with more moderate levels of scintillation occurring directly over the equator. Scintillation activity at higher latitudes tends to be more moderate than that near the equator. Greater temporal variability at high latitudes leads to different rms phase deviations and decorrelation times than for the same "intensity" of scintillation at lower latitudes. At solar minimum, scintillation activity in all three regions and at all frequencies is greatly reduced. Near the equator, 5 dB fades at L band are fairly uncommon. The most severe region tends to be the polar cap, where 5 dB fades can occur in patchy regions about 10% of the time. During solar minimum, rms phase deviations (at 250 MHz) rarely exceed 1 rad. For each of the plots shown in Figure 13, it should be noted that the scintillation levels at high latitudes are well correlated with occurrences of geomagnetic activity, while the lower latitude scintillation occurrences are not well correlated with geomagnetic activity.

2.5 MAGNETOSPHERIC PLASMAS

The high-latitude ionosphere is strongly linked to the magnetosphere by the geomagnetic field, and the variations of the high-latitude ionosphere are mainly driven by geomagnetic activity whose origins lie within the magnetosphere. Figure 14 shows a noon-midnight meridian cross-section (Rosenbauer et al., 1975) of the typical configuration of the geomagnetic field within the magnetosphere. The interaction of the solar wind, which flows at supersonic speeds (250-800 km/sec) relative to the Earth, with the magnetosphere causes the formation of a bow shock at distances of ~20 Earth radii upstream in the solar wind. The region of hot compressed solar plasma between the bow shock and the boundary of the magnetosphere (the magnetopause) is known as the magnetosheath. The size of the magnetosphere varies greatly, and is mainly determined by a balance between solar wind dynamic pressure and the magnetic pressure within the magnetosphere. The relative shape of the magnetosphere does not vary greatly with varying

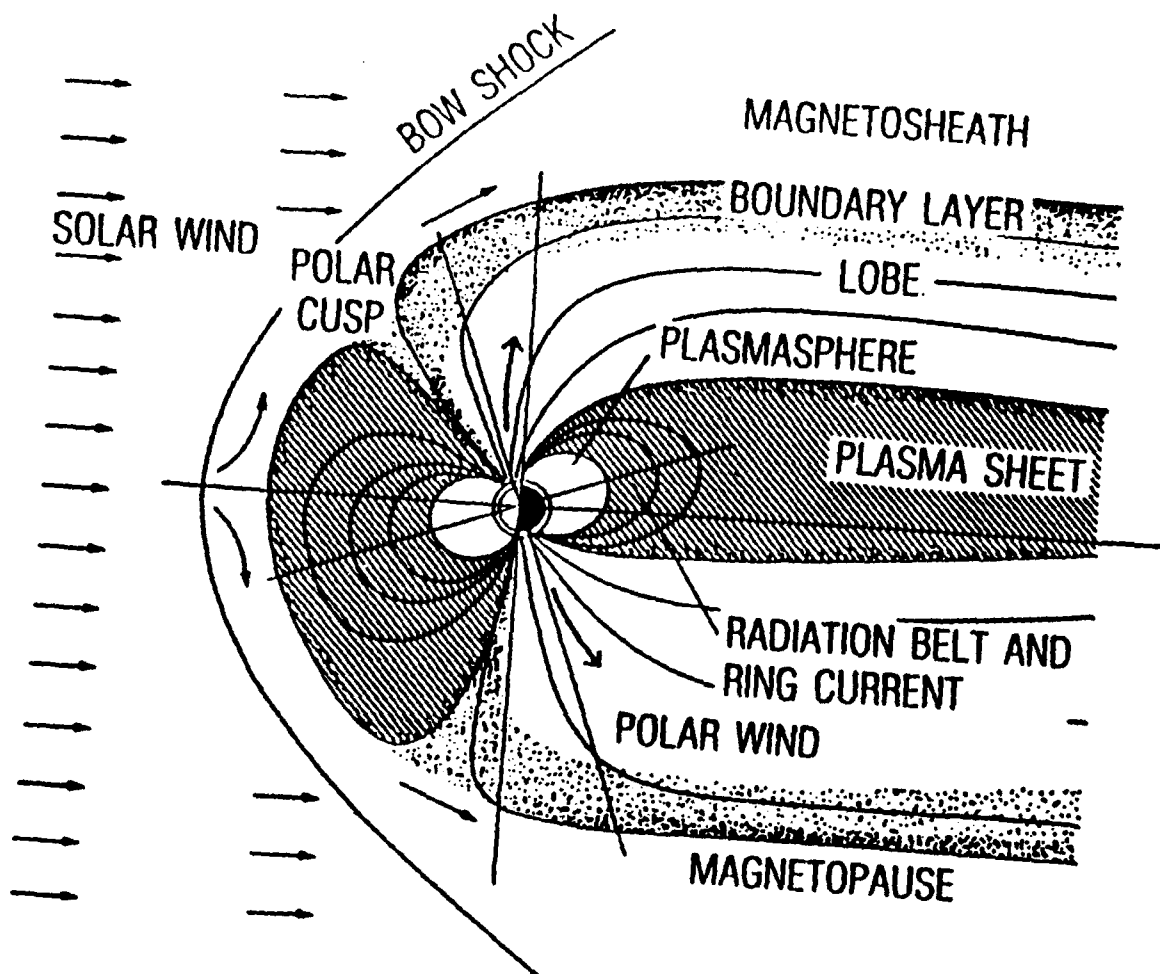


Figure 14. A Meridional View of the Earth's Magnetosphere Showing the Key Plasma and Energetic Particle Populations Which Respond to Variations in Solar Wind Parameters (from Rosenbauer, 1975).

solar wind conditions, although instabilities which lead to large-scale wave formation on the magnetopause have been identified. The magnetospheric tail, which extends hundreds of Earth radii downstream (well beyond lunar orbit), results from tangential forces of the solar wind along the magnetopause. The magnetotail is a poorly explored region of the magnetosphere, within which much of the magnetospheric plasma energization is initiated. Generally speaking, the outer portions of the magnetosphere are the most dynamic and are most strongly affected by variations in solar wind conditions. These outer regions magnetically "map" down into the ionosphere (i.e., following geomagnetic lines of force) at very high latitudes. The inner radiation belts, which contain the most energetic and penetrating trapped radiation in the magnetosphere, do not respond significantly to the external solar wind effects. The inner portions of the magnetosphere map into the ionosphere at low latitudes, and these regions do not exhibit large responses to changes in geomagnetic activity.

The interaction of the solar wind with the magnetosphere is energetically quite inefficient; it has been estimated that less than one percent of the incident solar wind energy flux is ultimately dissipated within the magnetosphere (Hill, 1981). The solar wind energy couples into the magnetosphere more effectively when the interplanetary magnetic field (IMF) has a large component in a direction opposite to that of the geomagnetic field. The solar wind-magnetosphere interaction sets up a large-scale convection pattern within the magnetosphere. Periods of "southward" IMF and high solar wind velocities are well correlated with enhancements of magnetospheric convection velocities. The magnetospheric plasma drifts in a circulation pattern from the dayside "cusp" region tailward over the polar caps into the tail "lobes" through the plasma sheet, where it becomes nonadiabatically energized, then sunward again (being adiabatically energized as it encounters higher magnetic field strengths nearer the Earth) until the plasma finally exits the dayside magnetopause. The convection cycle is completed in about 12-20 hours. Periods of enhanced activity result in enhanced fluxes of hot plasma within the magnetosphere, and

enhanced rates of precipitation of plasma into the high-latitude ionosphere and atmosphere.

The plasma sheet which forms amidst this convection process contains hot plasma which can cause electrical charging of the surfaces of satellites, particularly those in geosynchronous orbits (see DeForest, 1972; Mizera and Boyd, 1983). The earthward edge of the plasma sheet penetrates well inside of geosynchronous orbit during relatively high levels of geomagnetic activity. As plasma sheet particles drift earthward from the magnetotail, electrons tend to drift eastward (toward dawn) while ions drift westward (toward dusk). The most severe satellite surface charging events (and resulting electrostatic discharges) tend to occur in the midnight-to-dawn local time sector, where satellites encounter high fluxes of hot, drifting plasma-sheet electrons. The probability of occurrence and the severity of spacecraft charging events are directly correlated with periods of enhanced geomagnetic activity (Mizera and Boyd, 1983), corresponding to periods of enhanced convection and plasma-sheet energization. Severe spacecraft charging events tend to occur during the equinox seasons, when geosynchronous satellites enter and exit Earth eclipse once each day (also, geomagnetic storms show seasonal modulation; see Allen, 1984). In sunlight, photoelectron flux emitted from the satellite tends to balance current from the surrounding plasma. During eclipse, these vehicles cannot emit a photoelectron flux to balance the hot electron current from the plasma ($\sim 1\text{--}10 \mu\text{A}/\text{m}^2$), and electrical charging of the vehicles to several kilovolts is possible. Upon exiting eclipse, various surface materials discharge at different rates, creating the possibility of large differential potentials and discharges between external satellite components.

At altitudes below geosynchronous orbit, plasma motion is dominated by the effects of the Earth's rotation. Low energy (thermal) electrons and ions execute more-or-less circular trajectories around the Earth. The plasma trajectories are closed in the sense that the particles do not escape from the magnetosphere in steady-state conditions. The dominant source of low energy plasma in this corotating region is the ionosphere. The corotating region is known as the plasmasphere, and its outer boundary

is called the plasmapause. Because the drift paths within the plasmasphere are closed and stable, relatively high plasma densities can develop there (equatorial densities of $100\text{--}1000\text{ cm}^{-3}$ can occur within the plasmasphere, compared with densities of $0.1\text{--}10\text{ cm}^{-3}$ in the outer magnetosphere). Although the plasmaspheric plasma does not have significant direct effects on spacecraft systems, the enhanced plasma densities do affect communications (for example, up to 10 percent of the total column electron content in a surface-to-geosynchronous radio propagation path can be due to plasmaspheric plasma). Also, the high plasma densities within the plasmasphere tend to modify the rates at which high-energy radiation-belt particles are scattered into the ionosphere. Thus, the distribution of low energy plasma can affect other magnetospheric and ionospheric particle populations through secondary processes.

The radial position of the plasmapause is determined by the relative strengths of the electric fields associated with magnetospheric convection (variable) and the Earth's rotation (constant). During geomagnetically quiet conditions the plasmasphere can extend outward beyond geosynchronous orbit. During disturbed conditions the outer portions of the plasmasphere are swept away by enhanced magnetospheric convection, and the plasmasphere might extend only one quarter of the distance to geosynchronous orbit. The erosion of the outer plasmasphere during geomagnetic disturbances can occur within an hour of the onset of enhanced convection, while the refilling of the plasmasphere can take days. Thus, the distribution of plasma tends to be quite variable, and the shape of the plasmasphere depends both on the strength and on the time-history of geomagnetic activity.

2.6 MAGNETOSPHERIC ENERGETIC PARTICLES

During extended intervals of enhanced geomagnetic activity, large fluxes of trapped penetrating electrons ($>$ several hundred keV) can develop within the outer electron zone and near geosynchronous altitudes. These penetrating electrons can become embedded within bulk dielectrics on satellites (e.g., cable insulation, printed circuit boards) building up electrical potentials over time which can exceed the breakdown potential of the

dielectric (Meulenberg, 1976; Vampola, 1987). Theoretical and experimental results (Wenaas, 1977; Beers, 1977) have shown that breakdowns occur when the integrated fluence of penetrating electrons exceeds about 10^{12} cm^{-2} in time periods shorter than the leakage timescales of the dielectric (typically, several hours). These fluence levels are often exceeded in geosynchronous orbit over the several-day period following major geomagnetic storms. While the bulk-charging phenomenon can be eliminated through the use of modest shielding (Vampola, 1987), external unshielded cables are used on many satellites nevertheless. Weak discharges resulting from bulk charging can cause spurious signals in the affected circuitry while more severe discharges can damage some semiconductors. While surface charging events tend to be isolated to the region of drifting plasma-sheet electrons in the midnight-dawn local time sector, bulk charging tends to occur at all local times because the penetrating electrons tend to be distributed more uniformly and because the phenomenon is a cumulative effect. Other effects of enhancements of the trapped energetic particle environment include spurious signals in some space-based sensors, including silicon CCD arrays, photomultipliers and HgCdTe IR sensors (see Vampola, 1989), and enhanced heat loads (up to 0.5 Watts/m^2) on passive radiators (see Vampola et al., 1989).

The effects of the solar cycle on the Earth's energetic trapped particle environment were reviewed thoroughly in a recent paper by Vampola (1989). To a large extent, variations in the Earth's trapped energetic particle environment caused by solar activity are characterized well by the variations of geomagnetic activity (discussed in a previous section of this report) driven by solar activity. For example, fluxes of -MeV electrons in the outer zone of the Earth's radiation belts are known to increase by as much as two to three orders of magnitude in response to a geomagnetic storm (see Vampola, 1972). These flux increases can last up to two to three weeks following the geomagnetic storm occurrence. Variations of the trapped energetic electron environment maximize in the heart of the outer zone, near $-3.5 R_e$ radial distance, but modest fluctuations can be observed deeper in the radiation belts in response to the most extreme geomagnetic storms.

Energetic particle populations near geosynchronous orbit ($6.6 R_E$) are known to be influenced greatly by the occurrence of geomagnetic storms (see Paulikas and Blake, 1979; Baker et al., 1986; Nagai, 1988). At the onset of a geomagnetic storm, the energetic electron population is decreased rapidly by the combined effects of enhanced precipitation and by gross changes in the morphology of the magnetic field in the outer magnetosphere. Thus, one of the first effects of a geomagnetic storm onset is an energetic electron flux decrease. However, major storms produce enhanced fluxes of energetic electrons in the outer zone (internal to geosynchronous orbit). These particles can diffuse radially outward during and following the storm, leading to greatly enhanced fluxes of energetic electrons at geosynchronous orbit for several days following a major storm. Indeed, the regularity of this temporal behavior of electron flux in response to geomagnetic activity has been used to construct predictive techniques for estimating electron flux based on real-time indices of geomagnetic activity (see Nagai, 1988). Since this particle population is influenced so directly by geomagnetic storm occurrence, the variation of the particle population over the solar activity cycle should follow the expected trends for geomagnetic activity.

3. FORECASTS FOR SOLAR CYCLE 22

The previous sections of this report summarized the effects of solar activity on various aspects of the near-Earth space environment and the concomitant effects on man-made systems operating within that environment. Many parameters of the Earth's atmosphere, ionosphere, and magnetosphere respond either directly or indirectly to enhanced solar activity; sometimes in a manner which affects operational systems, and sometimes to a degree such that day-to-day life can be affected. Our current level of understanding of the relationships between solar activity and the near-Earth space environment is derived from historical data. It is only natural, especially from a practical or engineering viewpoint, to ask what conditions might be expected in the future. Fortunately, the sun has exhibited substantial (though not total) regularity in the ~11 year modulation of its activity over at least a few centuries (see Figure 1). This regular modulation has been sufficiently repeatable for many authors to identify clear temporal patterns in the activity cycles which can form the basis for statistical predictions of future activity. Unfortunately, the cycle-to-cycle coherence of the magnitude of solar activity has not been high enough to yield predictive capabilities with very high confidence levels. Furthermore, some evidence exists for very-long-term trends in solar activity, leading some to believe that we are viewing a continually changing sun (see, for example, Eddy, 1978; Wilson, 1984). Perhaps most importantly, however, virtually all of the predictive capabilities which have been published to date (with the exception of a few techniques based on the solar model described qualitatively by Babcock, 1961) are statistically based rather than physically based. That is, they rely on observed patterns in the data rather than on a quantitative understanding of the physical mechanisms which cause the modulation of solar activity.

Withbroe (1989) provided a review of solar activity predictions for cycle 22 based on data which were available about one year preceding the expected activity maximum in 1990. In his review, Withbroe characterized

predictive techniques as either "statistical" (i.e., relying on periodicities and trends observed in the long-term data set) or "precursor" (i.e., relying on observed patterns of activity, but updated with data representing the present or preceding cycle of activity). In evaluating the "confidence" which might be placed in predictions for cycle 22 based on several published techniques, Withbroe presented a figure (see also Brown and Simon, 1986) showing the actual performance of these techniques for "predicting" the maximum sunspot number for the preceding cycle (cycle 21). Not surprisingly, the statistical techniques, which weight historical data equally with recent data, tended to provide results which were near the long-term mean (since the mid-1800's, the long term mean of R_{\max} is about 116). The precursor techniques, which weighted recent data heavily, provided generally better results, but still demonstrated a substantial uncertainty. Overall, the predicted values of the maximum sunspot number for cycle 21 encompassed a range comparable to the complete range of values ever observed (i.e., from a low of about 30 to a high of about 200). In retrospect, the precursor techniques performed best, but the set of predictions based on precursor techniques still bracketed a range of approximately ± 50 about the actual observed value.

Predictions for the maximum of solar cycle 22 (see Withbroe, 1989; Brown, 1988; Kane, 1987; Lantos and Simon, 1987; Sargent, 1978; Schatten and Sofia, 1987; Wilson, 1984, 1988a,b; Brown and Simon, 1986) range from a low of about 40 to a high of around 200. There seems to be some consensus among the precursor techniques in predicting a sunspot maximum exceeding 170 with typical uncertainties of about ± 40 , implying that solar cycle 22 could be one of the 2 largest on record. Including data through January 1990, smoothed sunspot numbers for cycle 22 had already exceeded all but those of cycle 19.

Naturally, predictions which are performed for relatively short-time ranges (on the order of one year or less) are considerably more successful than long-term predictions. A specific example of the performance of the McNish-Lincoln technique (McNish and Lincoln, 1949) for solar cycle 21 and

the beginning of cycle 22 is shown in Figure 15 (from Solar-Geophysical Data Prompt Reports, Number 543, distributed by the NOAA National Geophysical Data Center). The McNish-Lincoln technique is based on the assumption that the expected value of the smoothed sunspot number at any phase in the present solar cycle is equal to the mean of all previous values observed for the same relative epoch modified by a correction factor which is proportional to the deviations from the means which have been observed for all previous months in the present cycle. Figure 15 plots the results of the McNish-Lincoln prediction scheme for a 1-year look-ahead. The figure shows observed smoothed sunspot values for all of cycle 21 and the beginning of cycle 22, along with the predicted values. Also shown is the mean of cycles 8 through 21. The performance of the prediction scheme was remarkably good for cycle 21: Typical deviations from observed values were less than 20. In particular the maximum value and time of maximum were predicted very well. The McNish-Lincoln scheme predicts a maximum of about 194 for cycle 22, with the maximum occurring in early 1990. If this prediction holds, cycle 22 would be the second largest on record, closely rivaling cycle 19 for the most extreme. Note that the uncertainties in the predicted maximum, even for a 1-year prediction, are still about ± 35 .

Even based on observed values as of January 1990, cycle 22 already ranks as the second largest ever observed. It is quite interesting to note that the three largest cycles on record (cycles 19, 22, and 21) have occurred very recently. It is unclear whether this represents a long-term trend toward increasing activity, a peak in a long periodic behavior, or simply a statistical excursion.

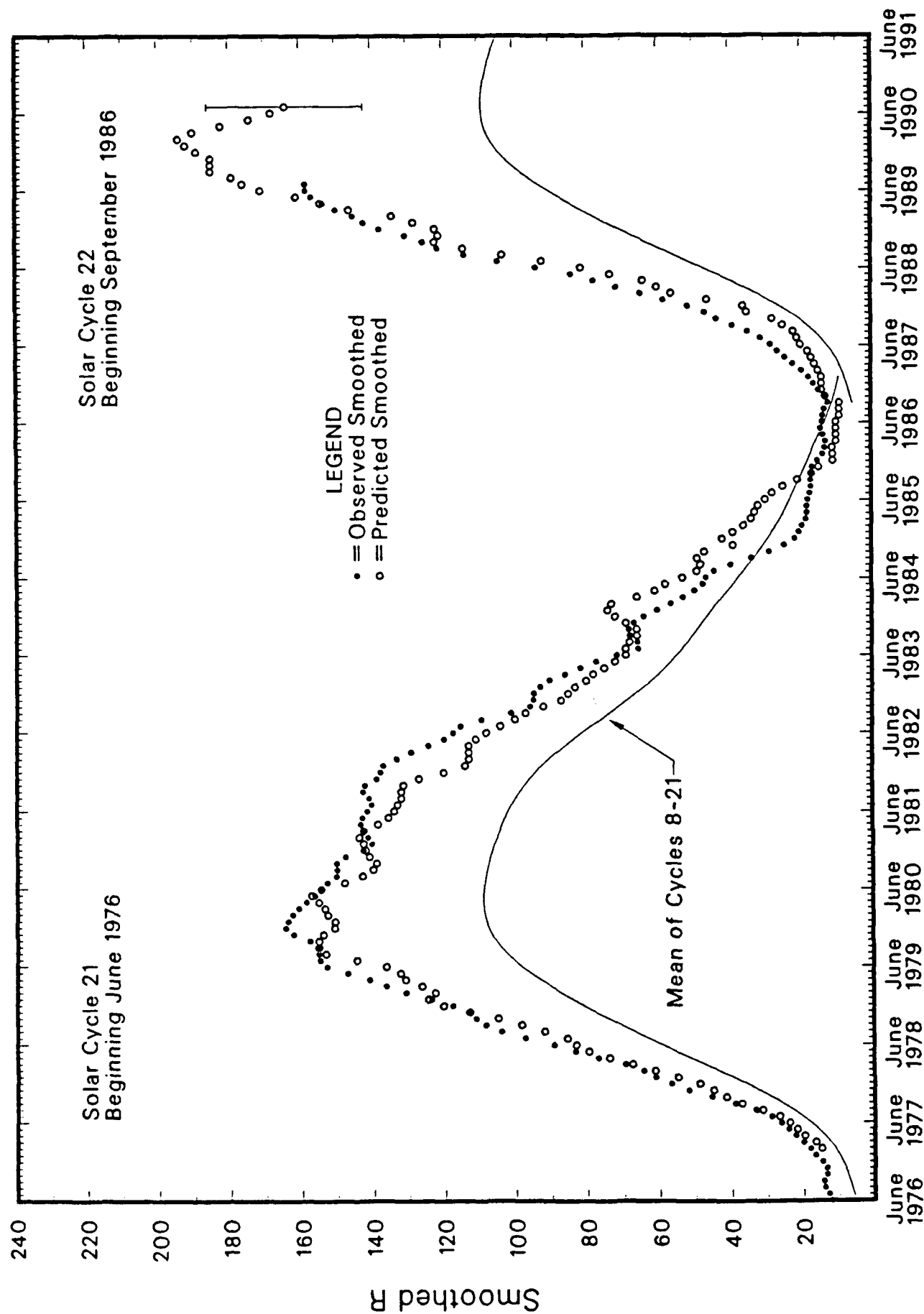


Figure 15. A Plot of Observed Smoothed Sunspot Numbers (Solid Circles) Compared to Values Predicted Using the McNish-Lincoln Technique (Open Circles). The solid line represents the mean for all cycles for which systematic data are available. The plot includes data through November 1989 (from the Solar-Geophysical Data Prompt Reports published by the NOAA National Geophysical Data Center).

4. SUMMARY

The observed rate of increase in solar activity at the initiation of solar cycle 22 has led to the anticipation that the activity during the solar maximum years, 1990-1991, may be the most severe of any period during the space age. Solar activity has many effects on man-made systems in space, on ground or aircraft communications, and on communications systems that penetrate the ionosphere. The effects of solar activity include prompt, direct effects which result from enhanced levels of solar UV, x rays and energetic particles, and the indirect effects of enhanced geomagnetic activity caused by the interaction between the solar wind and the terrestrial magnetosphere-ionosphere-atmosphere system. Energetic particle events are examples of solar activity which can affect humans in space or in high-flying aircraft. Also, enhanced solar activity causes changes in the terrestrial environment. Interactions between man-made systems and the disturbed local environment account for the majority of solar effects on these systems. The most prominent effects on space-based systems include electrostatic discharges which result from the interaction between satellites and the magnetospheric plasma and penetrating radiation environment; single event phenomena which result from solar particle impacts within microelectronic devices; enhanced sensor backgrounds due to elevated fluxes of trapped energetic particles; satellite drag due to atmospheric heating; and communication and tracking problems related to ionospheric disturbances.

Disturbances in the near-Earth plasma environment are tied closely to solar wind characteristics. Statistical data, case studies, and theoretical results indicate that the solar wind speed is the most important factor which affects geomagnetic activity over long time scales. This is an important result because the occurrence of high-speed solar wind streams is well correlated statistically with other observable aspects of solar activity such as sunspots. The interplanetary magnetic field, which does not have a strong correlation with the solar cycle, has been shown to correlate

well with geomagnetic disturbances on short time scales. Many empirical and theoretical relationships exist which provide quantitative measures of the influence of these solar wind parameters on geomagnetic activity levels, but few of the results offer a long term predictive capability for the upcoming cycle.

For practical purposes, such as estimating the effects of solar activity on operational space systems (e.g., estimating the expected incidence of severe-surface or bulk-charging events), or on communications systems (e.g., estimating the expected occurrences of severe "fades"), a method for predicting severe individual geomagnetic "events" may be more useful than relationships which correlate time-averaged geophysical parameters. Unfortunately, consistently successful geomagnetic event prediction on the basis of solar observations is not yet state of the art. Moreover, long-term predictions generally are statistically based and produce probabilistic results. However, it is clear from historical data that if solar activity during solar cycle 22 reaches extreme levels, then geomagnetic activity and its related effects also will exhibit historical levels during and for a few years after the solar maximum years. Indeed, the great geomagnetic storm of March 1989 and the solar proton events during August, September, and October 1989 are already clear indications of the historical importance of solar cycle 22. The occurrences of these events in the year preceding the expected solar maximum in 1990 may be the best evidence for predicting continuing high levels of geomagnetic and solar particle activity in the early 1990s.

This review is an admittedly peripheral review of a field which is broad, complex, and multidisciplinary. Furthermore, rapid developments in both the level of solar activity and the scientific community's understanding of that activity will very likely make many aspects of this review out of date at the time of printing. The author hopes that the review might expose the geophysics community to some interesting solar-terrestrial effects which affect John Q. Public.

REFERENCES

- B.-H. Ahn, H. W., Kroehl, Y. Kamide, D. J. Gorney, S. -I. Akasofu and J. R. Kan, "The Auroral Energy Deposition Over the Polar Ionosphere During Substorms," Planet. Space Sci. **37**, 239 (1989).
- S.-I. Akasofu, "Energy Coupling Between the Solar Wind and the Magnetosphere," Space Science Reviews **28**, 121 (1981).
- S.-I. Akasofu, "A Note on Variations of the IMF B_z and the AE Index Between 1966 and 1984 in Terms of Monthly and Yearly Averages," J. Geophys. Res. (submitted 1988).
- J. H. Allen, "Satellite Anomalies and Solar-Terrestrial Activity," in the Proceedings of the Spacecraft Anomalies Conference, ed. V. G. Patterson and J. S., Schleher, Colorado Springs (1984).
- J. Allen, H. Sauer, L. Frank, and P. Reiff, "Effects of the March 1989 Solar Activity," EOS, **70**, 1479 (1989).
- H. W. Babcock, "The Topology of the Sun's Magnetic Field and the 22-Year Cycle," Astrophysical Journal **133**, 572 (1961).
- D. N. Baker, L. F. Bargatze, and R. D. Zwickl, "Magnetospheric Response to the IMF: Substorms," J. Geomag. Geoelectr. **38**, 1047 (1986).
- D. N. Baker, J. B. Blake, R. W. Klebesadel, and P. R. Higbie, "Highly Relativistic Electrons in the Earth's Outer Magnetosphere, 1. Lifetimes and Temporal History 1979-1984," J. Geophys. Res. **91**, 4265 (1986).
- D. N. Baker, R. D. Zwickl, S. J. Bame, E. W. Hones, Jr., B. T. Tsurutani, E. J. Smith, and S.-I. Akasofu, "An ISEE 3 High Time Resolution Study of Interplanetary Parameter Correlations with Magnetospheric Activity," J. Geophys. Res. **88**, 6230 (1983).
- D. N. Baker, J. B. Blake, D. J. Gorney, P. R. Higbie, R. W. Klebesadel, and J. H. King, "Highly Relativistic Magnetospheric Electrons: A Role in Coupling to the Middle Atmosphere?," Geophys. Res. Lett. **14**, 1027 (1987).
- S. Basu, E. MacKenzie and S. Basu, "Ionospheric Constraints on VHF/UHF Communications Links During Solar Maximum and Minimum Periods," Radio Science **23**, 363 (1988).
- B. L. Beers, "Radiation-Induced Signals in Cables," IEEE Trans. Nucl. Sci. **NS-24**, 2429 (1977).

- G. M. Brown, "Solar Cycle 22 to be One of the Largest on Record?," Nature 333, 121 (1988).
- G. M. Brown, and P. A. Simon, "Long-Term Solar Activity Predictions," Solar-Terrestrial Predictions: Proceedings of a Workshop at Meudon, France, ed. P. A. Simon, G. Heckman, and M. A. Shea, NOAA, Boulder, CO (1986), pp. 1-6.
- L. F. Burlaga, K. W. Behannon, and L. W. Klein, "Compound Streams, Magnetic Clouds, and Major Geomagnetic Storms," J. Geophys. Res. 92, 5725 (1987).
- R. K. Burton, R. L. McPherron, and C. T. Russell, "An Empirical Relationship Between Interplanetary Conditions and Dst," J. Geophys. Res. 80, 4204 (1975).
- H. Carmichael, "Cosmic Rays (Instruments)," Annals of the IQSY, Vol. 1, pp. 178-197, MIT Press, Cambridge, MA (1968).
- D. L. Chenette and W. F. Dietrich, "The Solar Flare Heavy Ion Environment for Single Event Upsets," IEEE Transactions on Nuclear Science, Vol. NS-31, 1217 (1984).
- H. E. Coffey, editor, Solar-Geophysical Data, Part II: Comprehensive Report, 543, 114-126 (November, 1989).
- H. L. Collin, W. K. Petersen, and E. G. Shelley, "Solar Cycle Variation of Some Mass Dependent Characteristics of Upflowing Beams of Terrestrial Ions," J. Geophys. Res. 92, 4757 (1978).
- W. R. Cook, E. C. Stone, and R. E. Vogt, "Elemental Composition of Solar Energetic Particles," Astrophysical Journal 279, 827 (1984).
- N. U. Crooker, J. Feynman, and J. Gosling, "On the High Correlation Between Long-Term Averages of Solar Wind Speed and Geomagnetic Activity," J. Geophys. Res. 82, 1933 (1977).
- N. U. Crooker, N. U. and G. L. Siscoe, "The Effect of the Solar Wind on the Terrestrial Environment," Physics of the Sun, Vol. 3, pp. 193-249, D. Reidel Publishing Company, Dordrecht, Holland (1986).
- K. Davies, Ionospheric Radio Propagation, Monogr. 80, Natl. Bur. of Stand., Gaithersburg, Md. (1965).
- S. E. DeForest, "Spacecraft Charging at Synchronous Orbits," J. Geophys. Res. 77, 561 (1972).
- R. F. Donnelly, "Temporal Trends of Solar EUV and UV Full-Disk Indices," Solar Physics 109, 37 (1987).

- J. A. Eddy, "Historical Evidence for the Existence of the Solar Activity Cycle," in The Solar Output and Its Variation, pp. 51-72, ed. O. R. White, Colorado Assoc. University Press, Boulder, CO (1977).
- J. A. Eddy, "Historical and Arboreal Evidence for a Changing Sun," in The New Solar Physics, pp. 11-33, ed. J. A., Eddy, Westview Press, Boulder, CO (1978).
- T. J. Elkins and C. M. Rush, "A Statistical Predictive Model of the Polar Ionosphere," Report AFCRL TR-0331, Air Force Cambridge Research Laboratory, Bedford, MA (1973).
- J. Feynman and N. U. Crooker, "The Solar Wind at the Turn of the Century," Nature 275, 626 (1978).
- J. Feynman and S. M. Silverman, "Auroral Changes During the Eighteenth and Nineteenth Centuries and Their Implications for the Solar Wind and the Long-Term Variation of Sunspot Activity," J. Geophys. Res. 85, 2991 (1980).
- J. Feynman, "Implications of Solar Cycle 19 and 20 Geomagnetic Activity for Magnetospheric Processes," Geophys. Res. Lett. 7, 971 (1980).
- J. Feynman, "Geomagnetic and Solar Wind Cycles: 1900-1975," J. Geophys. Res. 87, 6153 (1982).
- J. Feynman, Comment on "Interplanetary Protons (EP = 1 MeV) 1973-1986 and Out to 22.4 AU," Geophys. Res. Letters 15, 840 (1988).
- J. Feynman, T. Armstrong, L. Dao-Gibner, and S. Silverman, "A New Proton Fluence Model for $E > 10$ MeV," Interplanetary Particle Environment, ed. J. Feynman and S. Gabriel, pp 58-71, Jet Propulsion Laboratory, Pasadena, CA (1988).
- J. Feynman and S. Gabriel, "New Model for Calculation and Prediction of Solar Proton Fluences," Proceedings of the 28th AIAA Aerospace Sciences Meeting, Reno, NV, 8-11 January (1990).
- J. Feynman and X. Y. Gu, "Prediction of Geomagnetic Activity on Time Scales of One to Ten Years," Reviews of Geophysics 24, 650 (1986).
- S. E. Forbush, "Three Unusual Cosmic Ray Intensity Increases Due to Charged Particles from the Sun," Physical Review 70, 771 (1946).
- S. E. Forbush, T. D. Stinchomb, and M. Scheim, "The Extraordinary Increase of Cosmic Ray Intensity on November 19, 1949," Physical Review 79, 501 (1950).
- G. Galilei, "Letters on Sunspots, 1612," in Discoveries and Opinions of Galileo, pp. 106-119, Doubleday and Company, Inc., New York (1957).

- H. B. Garrett, H. B., Dessler, A. J., and T. W. Hill, "Influence of Solar Variability on Geomagnetic Activity," J. Geophys. Res. 79, 4603 (1974).
- G. J. Gassman, Analog Model 1972 of the Arctic Ionosphere, Rep. AFCRL TR-0305, Air Force Cambridge Research Laboratory, Bedford, MA (1973).
- T. Gleissberg, "The Eighty-Year Solar Cycle in Auroral Frequency Numbers," J. Br. Astron. Assoc. 75, 227 (1965).
- G. Gloeckler, "Composition of the Energetic Particle Population in Interplanetary Space," Reviews of Geophysics 17, 569 (1979).
- W. D. Gonzalez and B. T. Tsurutani, "Criteria of Interplanetary Parameters Causing Intense Magnetic Storms," Planet. Space Sci. 35, 1101 (1987).
- W. D. Gonzalez, B. T. Tsurutani, A. L. C. Gonzalez, E. J. Smith, F. Tang, and S.-I. Akasofu, "Solar Wind-Magnetosphere Coupling During Intense Magnetic Storms (1978-1979)," J. Geophys. Res. 94, 8835 (1989).
- D. J. Gorney, "Solar Cycle Effects on Near-Earth Plasmas and Space Systems," J. Spacecraft and Rockets 26, 416 (1989).
- J. T. Gosling, J. R. Ashbridge, and S. J. Bame, "An Unusual Aspect of Solar Wind Speed Variations During Solar Cycle 20," J. Geophys. Res. 82, 3311 (1977).
- J. T. Gosling, J. R. Ashbridge, S. J. Bame, and W. C. Feldman, "Solar Wind Speed Variations: 1962-1974," J. Geophys. Res. 81, 5061 (1976).
- L. A. Hall, L. J. Heroux and H. E. Hinteregger, "Solar Ultraviolet Irradiance," in Handbook of Geophysics and the Space Environment, ed. A. S. Jursa, Air Force Geophysics Laboratory, Bedford, MA (1985).
- A. E. Hedin, "Correlations Between Thermospheric Density and Temperature, Solar EUV Flux and 10.7 cm Flux Variations," J. Geophys. Res. 89, 9828 (1984).
- T. W. Hill, Magnetospheric Boundary Layers, ESA-SP-148, European Space Agency, Paris, p. 325 (1981).
- H. E. Hinteregger, "AE-E Experiences of Irradiance Monitoring of 1250-1850 Å," Proceedings of the Workshop on Solar UV Irradiance Monitors, NOAA Environmental Research Laboratory, Boulder, CO (1980).
- J. W. Hirman, G. R. Heckman, M. S. Greer, and J. B. Smith, "Solar and Geomagnetic Activity During Cycle 21 and Implications for Cycle 22," EOS, 69, 962 (1988).

- J. Hirshberg, "The Solar Wind Cycle, the Sunspot Cycle and the Corona," Astrophys. Space Sci. 20, 473 (1973).
- A. J. Hundhausen, Coronal Expansion and Solar Wind, Springer-Verlag, New York (1972).
- A. J. Hundhausen, Coronal Holes and High Speed Streams, Colorado Assoc. Univ. Press, Boulder, CO (1977).
- J. R. Jasperse, "Sources and Characteristics of the Terrestrial Ionosphere," Physics of Space Plasmas, SPI Conference Proceedings and Reprint Series, Vol. 4, pp. 37-52 (1981).
- R. P. Kane, "Prediction of the Maximum Annual Mean Sunspot Number in the Coming Solar Maximum Epoch," Sol. Phys. 108, 415 (February 1987).
- T. L. Killeen, "Energetics and Dynamics of the Earth's Thermosphere," Reviews of Geophysics 25, 433 (1987).
- J. H. King, "Solar Proton Fluences for 1977-1983 Space Missions," J. Spacecraft and Rockets 11, 401 (1974).
- J. H. King, "Solar Cycle Variations in IMF Intensity," J. Geophys. Res. 84, 5938 (1979).
- P. Lantos and P. Simon, "Prediction of the Next Solar Activity Cycle," Proceedings of the 8th ESA Symposium on European Rocket and Balloon Programs and Related Research (ESA SP-270), pp. 451-453 (1987).
- M. A. Lee, "The Association of Energetic Particles and Shocks in the Heliosphere," Reviews of Geophysics and Space Physics 21, 324 (1983).
- M. A. Lee, "Acceleration of Particles at Solar Wind Shocks," The Sun and Heliosphere in Three Dimensions, ed. R. G. Marsden, Reidel, Dordrecht, Holland, p. 305 (1986).
- C. G. Little and H. Leinbach, "The Riometer - A Device for the Continuous Measurement of Ionospheric Absorption," Proceedings of the Institute of Radio Engineers 47, 315 (1959).
- J. L. Lloyd, G. W. Haydon, D. L. Lucas, and L. R. Teters, "Estimating the Performance of Telecommunications Systems Using the Ionospheric Channel," in Techniques for Analyzing Ionospheric Effects on HF Systems, Vol. 1, Institute for Telecommunication Services, Boulder, CO (1978).
- B. Lovell, "The Emergence of Radio Astronomy in the U.K. After World War II," Quarterly Journal of the Royal Astronomical Society 28, 1 (1987).

- K. Maezawa, Quantitative Modeling of Magnetospheric Processes, American Geophysical Union, Washington, DC (1979), p. 436.
- W. W. Maggs, "Biggest Solar Maximum Coming?," EOS, 69, 697 (1988).
- P. N. Mayaud, Derivation, Meaning and Uses of Geomagnetic Indices, Geophysical Monograph 22, American Geophysical Union, Washington, DC (1980).
- P. N. Mayaud, "Analysis of Storm Sudden Commencements for the Years 1868-1967," J. Geophys. Res. 80, 111 (1975).
- G. M. Mason, "The Composition of Galactic Cosmic Rays and Solar Energetic Particles," Reviews of Geophysics 25, 685 (1987).
- R. E. McGuire, T. T., von Rosenvinge, and F. B. McDonald, "The Composition of Solar Energetic Particles," Astrophysical Journal 301, 938 (1986).
- A. G. McNish and J. V. Lincoln, "Predictions of Sunspot Numbers," EOS, Transactions of the American Geophysical Union 30, 673 (1949).
- M. J. Mendillo, A. Klobuchar, R. B. Fritz, A. V. da Rosa, L. Kersley, K. C. Yeh, B. J. Flaherty, S. Rangaswamy, P. E. Schmid, J. V. Evans, P. Schodel, D. A. Matoukas, J. R. Koster, A. R. Webster, and P. Chin, "Behavior of the Ionospheric F Region During the Great Solar Flare of August 7, 1972," J. Geophys. Res. 79, 665 (1974).
- A. Meulenbergh, Jr., "Evidence for a New Discharge Mechanism for Dielectrics in Plasmas," Progress in Astronautics and Aeronautics: Spacecraft Charging by Magnetospheric Plasmas, Vol. 47, ed. A. Rosen, AIAA, New York, pp. 236-247 (1976).
- P. F. Mizera and G. Boyd, "A Summary of Spacecraft Charging Results," J. Spacecr. Rockets 20, 438 (1983).
- T. Murayama, Magnetospheric Study 1979, Japanese IMS Committee, Tokyo, p. 296 (1979).
- T. Nagai, "Space Weather Forecast: Prediction of Relativistic Electron Intensity at Synchronous Orbit," Geophys. Res. Lett. 15, 425 (1988).
- W. M. Neupert, and V. Pizzo, "Solar Coronal Holes as Sources of Recurrent Geomagnetic Disturbances," J. Geophys. Res. 79, 3701 (1974).
- H. W. Newton, "Sudden Commencements in the Greenwich Magnetic Records (1879-1944) and Related Sunspot Data," monthly Not. R. Astron. Soc. 5, 159 (1948).
- A. I. Ohl, "Physics of the 11-Year Variation of Magnetic Disturbances," Geomagn. Aeronomy 11, 549 (1971).

- S. Olbert, Physics of the Magnetosphere, D. Reidel Publishing Co., Dordrecht, Holland, p. 641 (1960).
- G. A. Paulikas and J. B. Blake, "Effects of the Solar Wind on Magnetospheric Dynamics: Energetic Electrons at the Synchronous Orbit," in Quantitative Modeling of Magnetospheric Processes, Geophysical Monograph No. 21, ed. W. P. Olson, p. 180, AGU, Washington, DC (1979).
- R. Roble, "Solar Cycle Variability of Global Mean Structure of the Thermosphere," in the Proceedings of the Conference on Solar Radiative Output Variability, ed. P. Foukal (1987).
- H. Rosenbauer, H. Grunwaldt, M. D. Montgomery, G. Paschmann and N. Sckopke, "Heos 2 Plasma Observations in the Distant Polar Magnetosphere: The Plasma Mantle," J. Geophys. Res. 80, 2723 (1975).
- C. T. Russell, "On the Possibility of Deducing Interplanetary and Solar Parameters from Geomagnetic Records," Solar Phys. 42, 259 (1975).
- H. H. Sargent, "A Prediction for the Next Solar Cycle," Proceedings of the 28th IEEE Vehicular Technical Conference, pp. 490-496 (1978).
- K. H. Schatten and S. Sofia, "Forecast of an Exceptionally Large Even-Numbered Solar Cycle," Geophys. Res. Lett. 14, 632 (1987).
- G. Schmidtke, "Modelling of the Solar EUV Irradiance for Aeronomic Applications," Encyclopedia of Physics, Vol. XLIX/7, Geophysics IV, Part VII, Springer-Verlag, p. 1-55 (1984).
- W. Schröder, "Aurorae During the Maunder Minimum," Meteorol. Atmos. Phys. 38, 246 (1988).
- H. Schwabe, "Solar Observations During 1843," Astronomische Nachrichten 21, 233 (1843).
- N. R. Sheeley, Jr. and J. W. Harvey, "Coronal Holes, Solar Wind Streams and Geomagnetic Disturbances During 1977 and 1978," Solar Phys. 70, 237 (1981).
- S. M. Silverman, "The Visual Aurora as a Predictor of Solar Activity," J. Geophys. Res. 88, 8123 (1983).
- J. A. Simpson, "Cosmic Radiation Neutron Intensity Monitor," Annals of the IGY, Vol. 4, p. 351-373, Pergamon Press, London (1957).
- D. F. Smart and M. A. Shea, "Galactic Cosmic Radiation and Solar Energetic Particles," Handbook of Geophysics and the Space Environment, ed. A. S. Jursa, Air Force Geophysics Laboratory, Bedford, MA (1985).

- D. F. Smart and M. A. Shea, "Proton Events During the Past Three Solar Cycles," J. Spacecraft and Rockets 26, 403 (1989).
- C. W. Snyder, Neugebauer, M., and U. R. Rao, "The Solar Wind Velocity and its Correlation with Cosmic Ray Variations and Geomagnetic Activity," J. Geophys. Res. 68, 6361 (1963).
- E. G. Stassinopoulos, "SOLPRO: A Computer Code to Calculate Probabilistic Solar Proton Fluences," NASA Goddard Spaceflight Center, NSSDC 75-11 (1975).
- Z. Svestka, Solar Flares, Geophysics and Astrophysics Monograph, 8, Reidel, Dordrecht, Holland (1976).
- T. F. Tascione, H. W. Kroehl, R. Creiger, J. W. Freeman, Jr., R. A. Wolf, R. W. Spiro, R. V. Hilmer, J. W. Shade, and B. A. Hausman, "New Ionospheric and Magnetospheric Specification Models," Radio Science 23, 211 (1988).
- R. J. Thompson, "The Rise of Solar Cycle 22," IPS TR-88-01, IPS Radio and Space Serv., Sydney (1988).
- M. R. Torr, P. G. Richards, and D. G. Torr, "A New Determination of the Ultraviolet Heating Efficiency of the Thermosphere," J. Geophys. Res. 85, 6819 (1980).
- A. L. Vampola, "Natural Variations in the Geomagnetically Trapped Electron Population," Proceedings of the National Symposium on Natural and Manmade Radiation in Space, ed. E. A. Warman, NASA TM-X-2440, pp. 539-547 (1972).
- A. L. Vampola, "Thick Dielectric Charging on High-Altitude Spacecraft," Journal of Electrostatics 20, 21 (1987).
- A. L. Vampola, "Solar Cycle Effects on Trapped Energetic Particles," J. Spacecraft and Rockets 26, 416 (1989).
- A. L. Vampola, R. D. Jimenez and J. E. Cox, "Heat Loads Due to the Space Particle Environment," J. Spacecraft and Rockets 26, 474 (1989).
- J. T. Visentine, editor, Atomic Oxygen Effects Measurements for Shuttle Missions STS-8 and 41-G, NASA TM-100459 (1988).
- R. R. Vondrak, G. Smith, V. E. Hatfield, R. T. Tsunoda, V. R. Frank, and P. D. Perreault, "Chatanika Model of the High-Latitude Ionosphere for Application to HF Propagation Prediction," Report 6056, RADC-TR-78-7, SRI Int., Menlo Park, CA (1978).
- R. A. Wagner, "Modeling the Auroral E Layer, Report AFCRL TR-0305, Air Force Cambridge Research Laboratory, Bedford, MA (1972).

- N. Wakai, "Quiet and Disturbed Structure and Variations of the Nighttime E Region," J. Geophys. Res. 72, 4507 (1976).
- R. L. Walterscheid, "Solar Cycle Effects on the Upper Atmosphere: Implications for Satellite Drag," J. Spacecraft and Rockets 26, 439 (1989).
- E. P. Wenaas, "Spacecraft Charging Effects by the High Energy Natural Environment," IEEE Trans. Nucl. Sci., NS-24, p. 2281-2284 (1977).
- R. M. Wilson, "A Comparative Look at Sunspot Cycles," NASA TM-2325 (1984).
- R. M. Wilson, "An Alternative View of the Size of Solar Cycle 22," Nature 335, 773 (1988).
- R. M. Wilson, "A Prediction for the Maximum Phase and Duration of Sunspot Cycle 22," J. Geophys. Res. 93, 10011 (1988).
- R. M. Wilson, "On the Long Term Secular Increase in Sunspot Number," Solar Physics 115, 397 (1984).
- G. L. Withbroe, "Solar Activity Cycle: History and Predictions," J. Spacecraft and Rockets 26, 394 (1989).
- A. W. Yau, P. H. Beckwith, W. K. Petersen and E. G. Shelley, "Long-Term (Solar Cycle) and Seasonal Variations of Upflowing Ionospheric Ion Events at DE 1 Altitudes," J. Geophys. Res. 90, 6395 (1985).
- R. Zwickl and J. Kunches, "Energetic Particle Events Observed by NOAA/GOES During Solar Cycle 22," 1989 Fall AGU meeting.

GLOSSARY OF SPECIAL SYMBOLS

aa or AA	= 3-hour planetary geomagnetic index, derived from two antipodal stations
am	= 3-hour (mondial) geomagnetic index
ap or Ap	= 3-hour planetary geomagnetic index, derived from K_p
f_oE	= critical frequency of the ionospheric E layer
f_oF_1	= critical frequency of the ionospheric F_1 layer
f_oF_2	= critical frequency of the ionospheric F_2 layer
$F_{10.7}$	= solar radio flux at 10.7 cm wavelength
hmE	= altitude of the ionization peak in the ionospheric E layer
hm F_1	= altitude of the ionization peak in the ionospheric F_1 layer
n	= solar wind density
AE	= auroral electrojet index
AL	= auroral electrojet index (lower envelope)
AU	= auroral electrojet index (upper envelope)
B_x, B_y, B_z	= Cartesian components of the interplanetary magnetic field (IMF)
Dst	= hourly geomagnetic index derived from midlatitude stations
K_p	= 3-hour quasi-logarithmic planetary geomagnetic index
Q_E	= effective 15-minute geomagnetic index
R	= sunspot number
T	= local time
V	= solar wind speed
θ	= clock angle of the interplanetary magnetic field
ΣK_p	= 24-hour sum of K_p
x	= solar zenith angle

GLOSSARY OF SPECIAL SYMBOLS (Continued)

Subscripts

a	= auroral
o	= ordinary mode of radio propagation
p	= planetary
s	= solar

LABORATORY OPERATIONS

The Aerospace Corporation functions as an "architect-engineer" for national security projects, specializing in advanced military space systems. Providing research support, the corporation's Laboratory Operations conducts experimental and theoretical investigations that focus on the application of scientific and technical advances to such systems. Vital to the success of these investigations is the technical staff's wide-ranging expertise and its ability to stay current with new developments. This expertise is enhanced by a research program aimed at dealing with the many problems associated with rapidly evolving space systems. Contributing their capabilities to the research effort are these individual laboratories:

Aerophysics Laboratory: Launch vehicle and reentry fluid mechanics, heat transfer and flight dynamics; chemical and electric propulsion, propellant chemistry, chemical dynamics, environmental chemistry, trace detection; spacecraft structural mechanics, contamination, thermal and structural control, high temperature thermomechanics, gas kinetics and radiation; cw and pulsed chemical and excimer laser development, including chemical kinetics, spectroscopy, optical resonators, beam control, atmospheric propagation, laser effects and countermeasures.

Chemistry and Physics Laboratory: Atmospheric chemical reactions, atmospheric optics, light scattering, state-specific chemical reactions and radiative signatures of missile plumes, sensor out-of-field-of-view rejection, applied laser spectroscopy, laser chemistry, laser optoelectronics, solar cell physics, battery electrochemistry, space vacuum and radiation effects on materials, lubrication and surface phenomena, thermionic emission, photosensitive materials and detectors, atomic frequency standards, and environmental chemistry.

Electronics Research Laboratory: Microelectronics, solid-state device physics, compound semiconductors, radiation hardening; electro-optics, quantum electronics, solid-state lasers, optical propagation and communications; microwave semiconductor devices, microwave/millimeter wave measurements, diagnostics and radiometry, microwave/millimeter wave thermionic devices; atomic time and frequency standards; antennas, rf systems, electromagnetic propagation phenomena, space communication systems.

Materials Sciences Laboratory: Development of new materials: metals, alloys, ceramics, polymers and their composites, and new forms of carbon; nondestructive evaluation, component failure analysis and reliability; fracture mechanics and stress corrosion; analysis and evaluation of materials at cryogenic and elevated temperatures as well as in space and enemy-induced environments.

Space Sciences Laboratory: Magnetospheric, auroral and cosmic ray physics, wave-particle interactions, magnetospheric plasma waves; atmospheric and ionospheric physics, density and composition of the upper atmosphere, remote sensing using atmospheric radiation; solar physics, infrared astronomy, infrared signature analysis; effects of solar activity, magnetic storms and nuclear explosions on the earth's atmosphere, ionosphere and magnetosphere; effects of electromagnetic and particulate radiations on space systems; space instrumentation.